

# Nanoemulsions Based on Phosphatidylcholine for the Intraductal Treatment of Breast Cancer and the Delivery of Paclitaxel and a P-Glycoprotein Inhibitor

1. Dr. S. Sujatha\*, Professor, dept of Pharmaceutics,

2. Y. RATNAKUMARI, ASSO. PROFESSOR, DEPT OF PHARMACOGNOSY

3. V. LEELA LAKSHMI, Asso. Professor, DEPT OF Pharmaceutics

4. T. VINOD KUMAR, Asst. Professor, DEPT OF Pharmaceutical Analysis

5. Dr. M. SREENIVASULU, PRINCIPAL, NARAYANA PHARMACY COLLEGE

<sup>1,2,3,4,5</sup> NARAYANA PHARMACY COLLEGE, CHINTHA REDDY PALEM, NELLORE

**Abstract:** This research examined the intraductal administration and localised therapy of breast cancer by incorporating the cytotoxic drug paclitaxel with the P-glycoprotein inhibitor elacridar hyaluronic acid (HA)-modified nanoemulsions. We looked at adding either tributyrin or perillyl alcohol to the oil phase of the nanoemulsion to increase cytotoxicity. The size of the nanoemulsions was less than 180 nm, and their zeta potential was negative. Perillyl alcohol and tributyrin both enhanced the cytotoxicity of nanoemulsions in MCF-7 cells, but not in MDA-MB-231. Perillyl alcohol, however, decreased the stability of the nanoemulsion when the medications were present. In comparison to a nanoemulsion that contained just paclitaxel (P-NE), the simultaneous addition of paclitaxel and elacridar to HA- and tributyrin-containing nanoemulsions (PE-NETri) enhanced cytotoxicity and decreased IC<sub>50</sub> by 1.6 to 3-fold in MCF-7 and MDA-MB-231 cells. Additionally, this nanoemulsion resulted in a 3.3-fold decrease in MDA-MB-231 spheroids' vitality. P-glycoprotein in membranes might be inhibited by elacridar added to the nanoemulsion. The significance of HA was shown by the three-fold increase in retention of a fluorescent marker after in vivo intraductal delivery of the NE containing HA as opposed to a solution or nanoemulsion without HA. There were no histopathological alterations in the breast tissue caused by the nanoemulsion. These findings bolster the possible applicability of the nanoemulsion for the treatment of breast cancer locally.

**Keywords:** nanoemulsion; intraductal; breast cancer; paclitaxel; P-gp inhibition

## 1. Introduction

A quarter of all diagnosed instances of breast cancer are ductal carcinoma in situ (DCIS), which is defined as neoplastic lesions in the breast's ductal-lobular structures that do not invade the basal myoepithelial membrane [1]. DCIS care often follows an aggressive pattern, including surgery with or without breast conserving, long-term endocrinotherapy, and radiation, since it may advance to invasive forms and there are presently no prediction tools for this change [2]. Medication administration straight into the ducts is helpful to maximise local medication concentration and minimise systemic adverse effects since DCIS develops within the ducts. As a localised approach to treat breast cancer and to restrict and/or reverse the carcinogenesis process, intraductal medication administration has been suggested in preclinical and clinical investigations [3–6]. It also serves as chemoprevention in high-risk individuals. Although to a lesser extent than systemic administration, prior evidence indicated that small drugs are likely to diffuse into the systemic circulation after intraductal administration as solutions due to ductal permeability [7]. This can be problematic given the high toxicity of antitumor drugs. In addition to its ductal permeability, skilled professionals are needed for its cannulation during delivery. Therefore, in order to combine effectiveness, safety, and a reduction in the frequency of administration, methods to improve ductal retention of medications must be used [8]. Nanocarriers, including lipid nanoparticles, nanoemulsions, To meet this demand, delivery methods such as polymeric aggregates and nanosuspensions have been suggested [7–10]. Increases in the

molecular weight of PEG-polymer aggregates have been shown by Singh et al. to enhance retention in the ducts [7]. It has also been shown that ductal retention of micro and nanoparticles occurs, with 1 μm particles exhibiting longer retention than 100 and 500 nm nanoparticles [11]. Longer retention periods of a fluorescent dye were also obtained by administering an in situ gel as opposed to its solution, indicating the significance of viscosity and bioadhesion for local retention [11]. In contrast to solutions, our lab has previously shown that nanoemulsions containing bioadhesive polymers extended the retention of fluorescent markers in the mammary tissue [8,12]. In the current investigation, paclitaxel and elacridar were co-incorporated and delivered intraductally using hyaluronic acid (HA)-modified nanoemulsions with cytotoxic ingredients as the oil phase. Colloidal dispersions of two immiscible liquids, usually water and oil, stabilised by surfactants are called nanoemulsions. Nanoemulsions were selected as delivery systems due to several properties and advantages over other nanocarriers: (i) The oil phase aids solubilization of lipophilic compounds such as paclitaxel and elacridar while still enabling their dispersion in an aqueous external phase; (ii) the presence of a surfactant interface offers an additional area for incorporation of drugs with poor aqueous solubility; (iii) nanoemulsions can incorporate large amounts of water (>60%) and can be obtained with lower amounts of surfactants compared to other emulsified nanosystems, such as microemulsions, which generally result in a lower irritation potential; (iv) it is possible to modify the surface of the

droplets with ligands, improving cell internalization and selectivity, among other properties; and (v) several types of oil phases can be utilized for their production, and their selection can be based on their ability to dissolve the drug and/or to confer additional properties to the formulation (such as an improved cytotoxicity) [13–16]. Its affinity for the differentiation cluster protein 44 (CD44), a receptor overexpressed in several cancer types that has been proposed to help cancer cell targeting, and its bioadhesive qualities (to prolong mammary tissue retention) justify the use of HA in nanoemulsion modification [17]. In order to assist reverse multidrug resistance, we postulated that these nanoemulsions may increase paclitaxel cytotoxicity, extend breast tissue retention, and block the P-glycoprotein efflux transporter (P-gp).

A well-known cytotoxic medication called paclitaxel (P) has been used in the clinic to treat early and metastatic breast cancer. It has been shown to be more effective than doxorubicin and cyclophosphamide [18–20]. Its capacity to attach to  $\beta$ -tubulin, stabilise the polymerised microtubule, arrest the cell cycle in G2/M, and induce apoptosis is primarily responsible for its mode of action [21,22]. Its limited selectivity against tumour cells, which causes several negative side effects when given systemically, supports the decision to deliver it directly into the ducts [23]. Additionally, tumour resistance, which is often linked to overexpression of efflux proteins—particularly P-gp of the ABC family (ATP-binding cassette)—reduces the effectiveness of this medication [24, 25]. To overcome resistance development, the nanoemulsion was supplemented with elacridar (E). A strong inhibitor of P-gp and breast cancer resistance protein (BCRP), elacridar has the benefit of not being a substrate for P-gp and inhibiting it at concentrations 100 times lower than weak inhibitors like verapamil [26]. The capacity of elacridar to block the efflux transporter expressed in the skin was not hindered by its inclusion, since we have previously shown that its co-incorporation in nanoemulsions with P-gp substrates enhances drug retention in the epidermis [27]. Perilyl alcohol and tributyrin were investigated as additions to the nanoemulsion oil phase in order to further enhance the cytotoxicity of the nanoemulsion. By isoprenylating ras gene products and inhibiting the regulating function of nuclear factor kappaB (NF- $\kappa$ B) expression, perilyl alcohol has been shown to regulate cell proliferation and induce cell death without damaging normal cells [28–30]. Tributyrin is a prodrug of butyric acid and has been shown to have anticarcinogenic properties via caspase-3-dependent or -independent processes that include the up-regulation of Bax and the down-regulation of Bcl-2 [31]. To assist The addition of C6 ceramide to tributyrin-loaded nanoemulsions enhanced their cytotoxicity against MCF-7 cells, suggesting a potential function for tributyrin in enhancing cytotoxicity [8]. This study's first phase included optimising the composition of the nanoemulsion and examining how composition affected its physicochemical characteristics, stability, and cytotoxicity. Following that, the effects of nanoemulsions on P-gp inhibition and paclitaxel cytotoxicity were investigated in 2D and 3D breast cancer models using MCF-7 and MDA-MB-231 cells, which were chosen due to their unique expression of CD44, progesterone receptor (PR), oestrogen receptor (ER), and human epidermal growth factor receptor 2 (HER2). Because they mirror between 79% and 84% of cases, MCF-7 cells—which are ER+, PR+, HER2+, and CD44+—are often used as in vitro models for breast cancer [32]. The

ER-, PR-, HER2-, and CD44+++ MDA-MB-231 cells have been widely used as models for triple-negative breast cancer [33]. The absence of effective therapeutic options for triple negative breast cancer makes having increased cytotoxicity against MDA-MB-231 cells significant [34, 35]. Last but not least, the in vivo ability of a chosen formulation to extend local retention was evaluated.

## 2. Results

### *Nanoemulsion Development, Composition Selection, and Cytotoxicity*

In the first section of our investigation, we examined how different concentrations of tributyrin (Tri), hyaluronic acid (HA), and perilyl alcohol (PA) affected the characteristics of the nanoemulsion. Tricaprylin and tricaprolylin including either perilyl alcohol or tributyrin (varying from 0.5 to 5% as final concentration in the nanoemulsion) were the three kinds of oil phase that were tested in order to evaluate the effects of Tri and PA. Prior to the surfactant:oil phase mixture's aqueous phase addition, HA was dissolved in PBS to achieve final concentrations of 0.125, 0.25, and 0.5%. The objective was to maximise the amount of PA, tributyrin, and HA in the nanoemulsion while preserving its stability in order to optimise its composition. Following compositional definition, the cytotoxicity of a few chosen nanoemulsions in cell monolayers was compared. Impact of the Oil Phase on NE Features: Impact of PA and Tributyrin

First, we evaluated how the oil phase affected the properties of the nanoemulsion. The nanoemulsions did not include HA for this assessment. The generation of nanoemulsions with droplet diameters below 200 nm and PDI < 0.21 was made possible by PA at 1 and 2.5%, indicating a restricted sized distribution (Table 1). However, after five days, the NE containing 2.5% of PA became more viscous, which would make intraductal delivery difficult. A thick emulsion was produced instead of fluid systems when the PA content was increased to 5%. Similarly, replacing PA with tributyrin at 2.5 or 5% resulted in viscous emulsions; only at 1% did tributyrin permit the creation of fluid systems with droplets of around 100 nm (Table 1). The formulation that included tributyrin (NETri minus HA) had the lowest zeta potential of all the nanoemulsions. These findings imply that a tributyrin concentration of more than 1% prevented the production of nanoemulsions with the required properties for intraductal application. The nanoemulsions with 1% tributyrin or PA did not exhibit any distinct textures under a polarised light microscope that may be connected to aggregates, big droplets, or lamellar phase formation. These nanoemulsions were exposed to HA inclusion since their macroscopic and microscopic appearances remained unchanged for seven days.

**Table 1.** Influence of the type of oil phase on the droplet size, PDI and zeta potential of nanoemulsions without HA, and influence of the concentration of HA, paclitaxel (P) and elacridar (E) on the physicochemical characteristics of nanoemulsions containing perillyl alcohol (PA) or tributyrin (Tri).

Nanoemulsion	OilPhase/DrugConcentration	Size(d.nm)	PDI	ZetaPotential(mV)
NE(noHA)	Tricaprylin	164.3 ±7.8	0.178 ±0.02	-23.8±2.8
NETri	Tricaprylin+tributyrin(1%)	100.89±1.1	0.114 ±0.04	-41.7±1.8
(noHA)	Tricaprylin+tributyrin(2.5%)	-	-	-
NEPA	Tricaprylin+PA(0.5%)	175.1 ±1.8	0.204 ±0.11	-27.2±1.2
(noHA)	Tricaprylin+PA(1%)	139.4 ±0.9	0.192 ±0.01	-12.1±0.7
	Tricaprylin+PA(2.5%)	155.2 ±1.7	0.170 ±0.04	-17.7±2.2
	Tricaprylin+PA(5%)	-	-	-
E-NETri	Tricaprylin+tributyrin(1%)0.1%E	608.1 ±0.4	0.327 ±0.01	-19.9±3.1
(with0.25%HA)	Tricaprylin+tributyrin(1%)(0.07%E)	202.9 ±0.7	0.197 ±0.03	-17.5±1.8
PE-NETri	Tricaprylin+tributyrin(1%)0.07%E+1%P	228.9 ±1.0	0.459 ±0.01	-19.0±5.9
(with0.25%HA)	Tricaprylin+tributyrin(1%)0.07%E+0.5%P	114.6 ±1.2	0.292 ±0.01	-32.4±0.28
E-NEPA	Tricaprylin+PA(0.5%)0.1%E	329.2 ±8.7	0.216 ±0.02	-11.4±0.2
(with0.25%HA)	Tricaprylin+PA(0.5%)0.07%E	138.7 ±1.9	0.183 ±0.11	-15.1±1.5
PE-NEPA	Tricaprylin+PA(0.5%)(0.07%E+1%P)	216.0 ±14.8	0.413 ±0.06	-34.2±6.7
(with0.25%HA)	Tricaprylin+PA(0.5%)(0.07%E+0.5%P)	134.2 ±3.8	0.293 ±0.01	-26.0±1.4

#### Influence of HA Incorporation on NE Characteristics

To enhance the bioadhesive qualities and retention of mammary tissue, HA was added at a concentration of 0.125 to 0.5%. HA prevented the creation of homogenous nanoemulsions at 0.5%. All formulations using solely tricapyrylin as the oil phase (U-NE), tricapyrylin plus PA (NEPA1%), or tributyrin (NETri1%) at 1% (w/w) showed a diameter less than 180 nm, a PDI less than 0.22, and a negative zeta potential at 0.125 or 0.25% of HA (Figure 1A). After seven days, however, creaming was seen in the formulations with 1% PA but not tributyrin. The formulations reverted to their initial shape after shaking, however an increase in particle size and PDI (above 0.3) was seen, indicating the formulations containing 1% PA were not stable when HA was present. Formulations were steady for a week after the PA content was lowered to 0.5% (NEPA0.5%). The increase in HA concentration to 0.25% did not significantly ( $p > 0.05$ ) lower the potential when compared to any other nanoemulsions. These findings led to the selection of HA at 0.25% to enhance bioadhesion, and three different kinds of nanoemulsions were examined for further characterisation, cytotoxicity, and stability assessment: Tricaprylin with 0.5% PA and 0.25 HA (known to as NEPA), tricapyrylin with 1% tributyrin and 0.25% HA (referred to as NETri), or NE having solely tricapyrylina oil phase and 0.25% HA (referred to as U-NE).

#### Characterization of Selected Formulations

The rheological behaviour of the chosen nanoemulsions was further examined (Figure 1B). The low viscosity (below 0.005 Pa.s) of all formulations was justified by the fact that 80% of their content is water. The linear connection between shear rate and shear stress suggests Newtonian behaviour, suggesting that at the concentrations utilised, tributyrin and PA did not influence the nanoemulsion's other rheological behaviour, albeit PA seemed to encourage a minor rise in viscosity. Figure 1(C1) shows a representative picture of the tricapyrylin-containing nanoemulsion. It is evident that spherical droplets smaller than 200 nm were produced, supporting the diameter determined by light scattering. For the other nanoemulsions,

comparable pictures were acquired. Under the polarised light microscope, no bigger droplets or other textures were seen (Figure 1(C2)), indicating that the addition of PC to the surfactant mix did not result in the production of liquid crystalline bulk phases [36]. Additionally, because the intraductal route is parenteral and needs a pH as near to physiological pH as feasible to minimise local pain [38], the formulations' pH (around 6.7, as determined by pH strips) supports compatibility with the intended route [37].

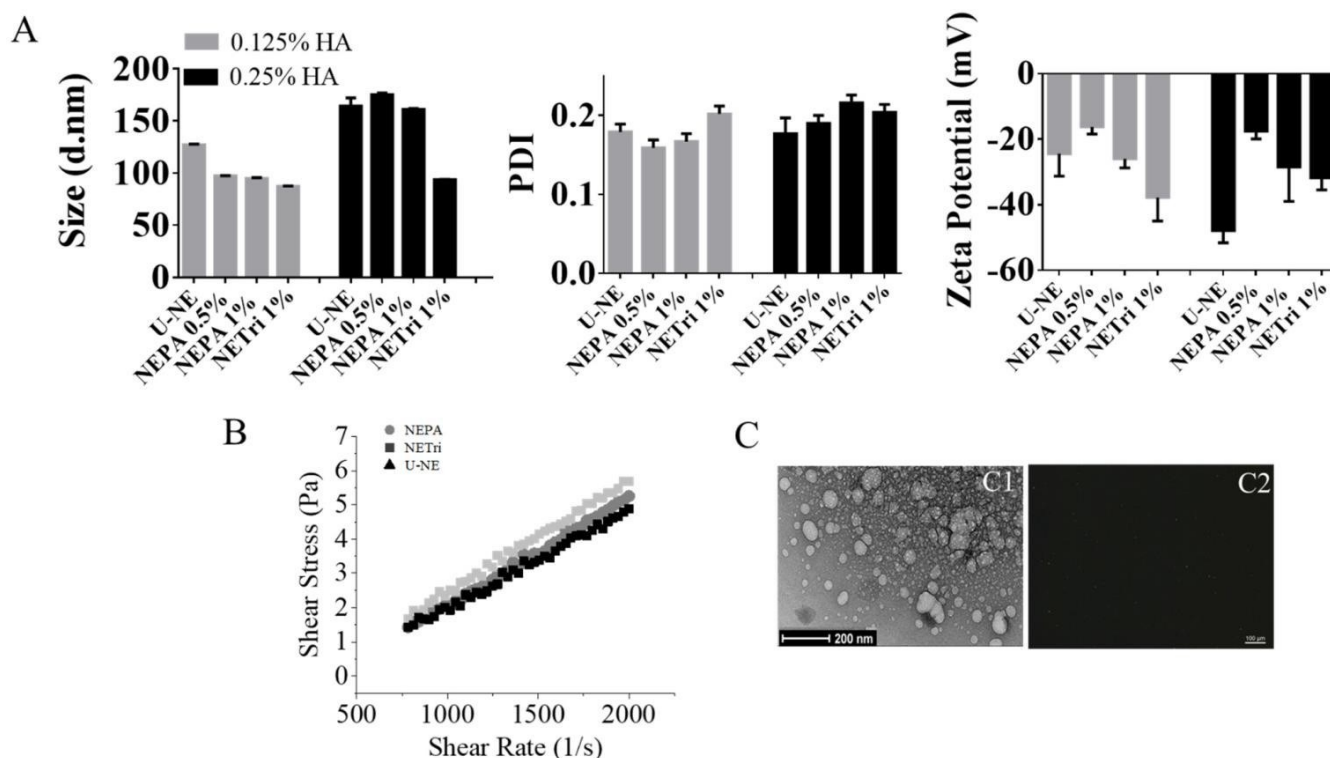


**Figure 1.** Nanoemulsion development and characterization. (A) Influence of NE composition (unloaded, containing perillyl alcohol or tributyrin) and HA concentration on the size distribution, polydispersity index (PDI), and zeta potential. (B) Rheological behavior of U-NE (NE containing only tricaprylin as oil phase and 0.25% HA), NEPA (NE containing tricaprylin with 0.5% PA and 0.25% of HA), and NETri (tricaprylin with 1% tributyrin and 0.25% HA). (C) Microscopy images of NETri. (C1) Representative image of transmission electron microscopy of NETri. (C2) Representative image of polarized light optical microscopy of the formulation. At least three batches of each formulation were produced.

**Influence of Nanoemulsion Composition on Its Cytotoxicity**  
After Tri, PA, and HA concentrations in the nanoemulsions were optimized, the chosen formulations were then tested for cytotoxicity in cell monolayers. Since (i) HA has bioadhesive qualities and is a ligand of CD44, which may influence interactions with cells and cytotoxicity, and (ii) tributyrin and perillyl alcohol have been reported to enhance the cytotoxic qualities of medications and formulations [8,16,29], the comparison of nanoemulsions with different compositions is justified.

By contrasting the NE-containing tricaprylin in the oil phase with and without HA at 0.25% (U-NE), the impact of HA addition was evaluated. At the maximum concentration used, the nanoemulsion without HA, tributyrin, or PA decreased the viability of MCF-7 cells to around 70%, whereas MDA-MB-231 cells showed a comparable impact at a lower dose (Figure 2). The components of unloaded nanoemulsions may be responsible for their cytotoxicity. It has been shown that surfactants, such as polysorbates, and elements of the oil phase of emulsified nanocarriers alter membrane permeability

and enhance the release of inflammatory cytokines, which in turn affects cell viability [39–42]. This may add to the overall cytotoxicity of drug-loaded nanoemulsions and is in line with the previously documented potential of nano and microemulsions to influence the viability of tumour and non-tumour cells based on the type/concentration of the oil phase and surfactants [43–46]. Cell viability was not significantly impacted by the presence of HA (Figure 2 and Table 2).



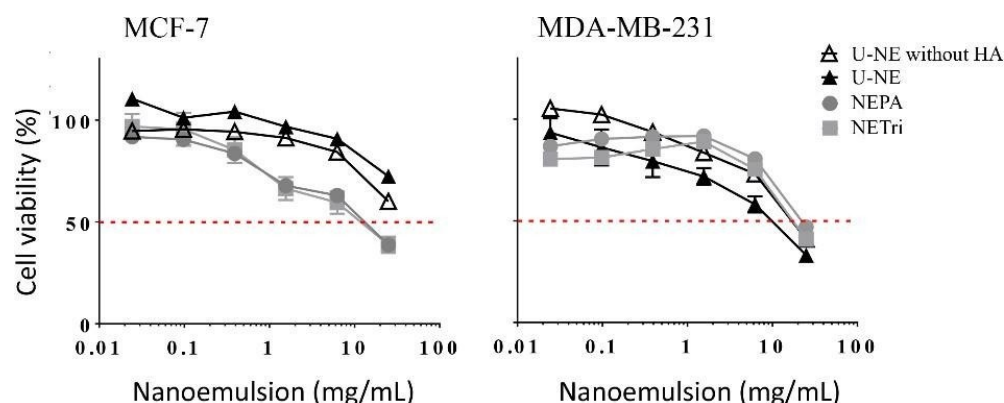


**Figure 2.** Influence of the concentration of U-NE, U-NE without HA, NEPA, and NETri on the viability of MCF-7 and MDA-MB-231 cells in monolayer (2D culture) after 48 h of treatment. Data are represented as the mean  $\pm$  SD,  $n=12-16$  in 3-4 separate experiments.

**Table 2.** Values of  $IC_{50}$  related to MCF-7 and MDA-MB-231 cell lines.

$IC_{50}$	MCF-7		MDA-MB-231	
	mg/mL of NE	$\mu$ M of P	mg/mL of NE	$\mu$ M of P
U-NE without HA	-	-	15.5	-
U-NE	-	-	6.6	-
NETri	9.7	-	8.2	-
NEPA	12.6	-	9.7	-
P-Sol	-	78.8	-	61.8
PE-Sol	-	66.0	-	62.4
P-NETri	4.7	27.4	0.9	5.0
PE-NETri	2.9	17.1	0.3	1.7

To evaluate the impact of adding tributyrin and PA, the cytotoxicity of NETri and NEPA (both of which contained 0.25% HA) was then evaluated. Despite having double the tributyrin content, these nanoemulsions showed equivalent  $IC_{50}$  values and comparable cytotoxicity in both cell lines (Figure 2, Table 2). Only in MCF-7 cells did NETri and NEPA have lower  $IC_{50}$  values than U-NE, which confirms earlier findings that adding tributyrin to nanoemulsions increases their cytotoxicity in MCF-7 cells [8] and shows that this effect can be obtained at a concentration that is about eight times lower than that previously used. Due to this improvement in cytotoxicity, NETri and NEPA were chosen to be included into paclitaxel.

#### *Influence of Paclitaxel and Elacridar Incorporation on Nanoemulsion Characteristics*

Elacridar (E) did not permit the generation of nanoemulsions with the required size at the highest concentration investigated (0.1%) (Table 1). Elacridar was not entirely dissolved in the surfactant:oil phase mixtures at this concentration, and only a small number of drug crystals were visible under a polarised light microscope. This might account for the droplet diameter increase of around 2.2-6 times. Its solubility and the acquisition of droplets smaller than 200 nm were made possible by lowering its concentration to 0.07% (Table 1). Paclitaxel (P) was likewise exceedingly difficult to solubilise at 1% in the surfactant:oil phase combination (which also included Eat 0.07%); independent of the presence of tributyrin or PA, the resultant nanoemulsions showed  $PDI > 0.4$  and sedimentation was seen after two days. The existence of two populations (seen in the DLS size distribution) and non-dissolved paclitaxel may be the cause of this high PDI (Supplementary Figure S1). Nanoemulsions with a more constrained size distribution were produced by lowering the paclitaxel concentration to 0.5%. When paclitaxel was added to NETri (PE-NETri), the droplet size was almost doubled in comparison to the nanoemulsions that contained just

elacridar (E-NE). While drugs may be able to alter the properties of PC-based systems [47]. We credit this decrease to a longer bath sonication (~10 min) for paclitaxel solubilisation, which may have enhanced formulation homogenisation overall. Instead of measuring drug trapping, we worked with the idea of "drug incorporation in the nanoformulation." Because of the presence of surfactant monomers, propylene glycol (which is incorporated in the surfactant blend but may partition into the aqueous phase), and the formation of other structures (as micelles due to the excess of surfactant), we thought that drug incorporation prevented drug precipitation by encasing the sum of the fractions of drug dissolved/entrapped into the oil droplets, in the surfactant interface, and dispersed/dissolved in the aqueous external compartment [48-50]. Previous research that documented an increase in the apparent solubility of APIs facilitated by "liposomalization" and/or "micellisation" [51] supports this. We took 100% integration into consideration since the chosen medication doses did not cause precipitation. The drug-loaded nanoemulsions were compared to the

unloaded formulations after undergoing a 90-day short-term stability testing. Every unloaded formulation had a size below 200 nm, a PDI between 0.11 and 0.20, and a zeta potential between -12 and -42 mV at the time of acquisition (Figure 3A). All formulations exhibit an increase in size after 90 days: around 21.5 nm for NETrian and 42.9 nm for NEPA. Although the formulation retained its macroscopic properties, the PDI of NEPA rose about 1.5 times, whereas the PDI values of NETri hardly altered (Figure 3A). There was no discernible creaming, phase separation, or coalescence, despite NETri exhibiting the most marked rise in Zeta potential. Stability was

impacted by drug incorporation, as shown in Figure 3B. An approximately 1.5-fold rise in PE-NEPA's zeta potential was seen after 90 days. According to reports, medication encapsulation and release over time may alter the droplet surface structure, which might alter the zeta potential by altering the orientation of the phosphatidylcholine head groups [52]. Furthermore, more noticeable alterations in droplet size and PDI of PE-loaded NEPA were seen, but not of PE-NETri, indicating that PE integration had an impact on NEPA stability. Therefore, only PE-NETri was investigated further.

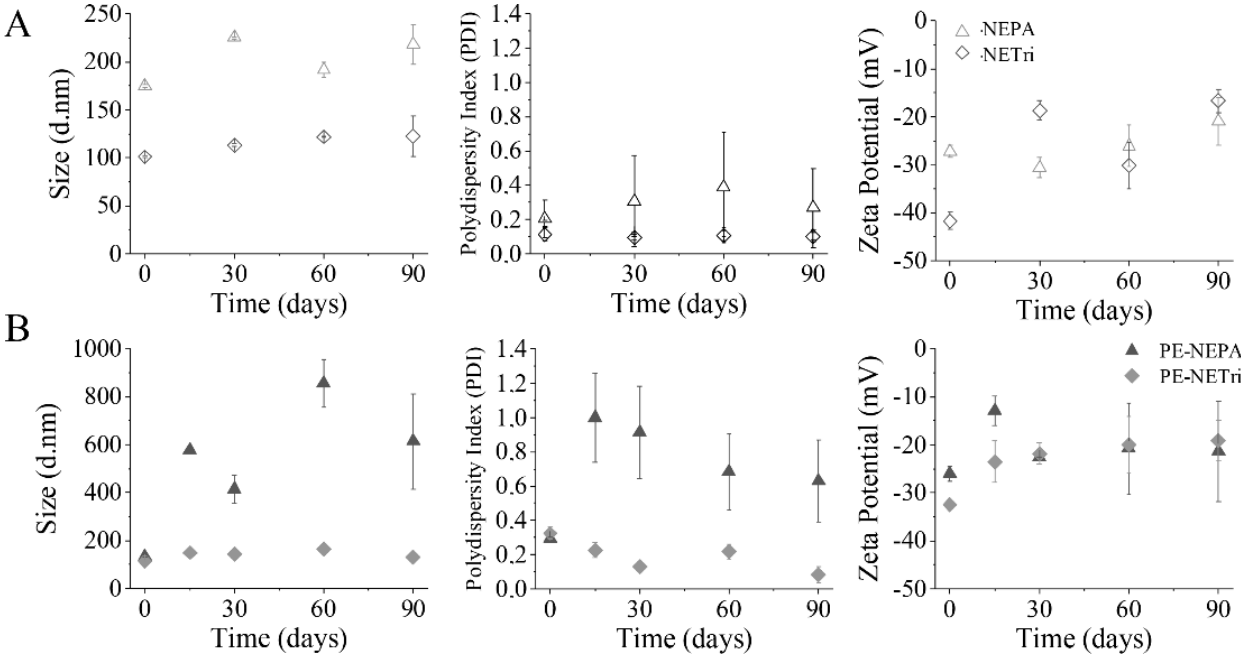


**Figure 3.** Nanoemulsion short-term stability. (A) Influence of NE composition (NEPA and NETri) on size distribution, polydispersity index (PDI) and zeta potential for 90 days. (B) Influence of NE loading with paclitaxel and elacridar (PE-NEPA and PE-NETri) on size distribution, polydispersity index (PDI) and zeta potential for 90 days. At least three batches of each formulation were analyzed.

After 30 days of storage at room temperature (kept by air conditioning set at 25 °C), shielded from light, a preliminary evaluation of the drug content in NETri was carried out (SupplementaryFigure S2A).The paclitaxel and elacridar content was more than 95%, indicating their stability throughout the course of the study.Furthermore, the release of paclitaxel and elacridar from NETri was investigated to make sure that, due to their lipophilia, the medications would not be kept in the emulsion for extended periods of time.At 24 hours, 78.2±12.4% of paclitaxel and 60.0±11.7% of elacridar were released from NETri. Release increased with time (Supplementary Figure S2B).Following data fitting, Higuchi's model was able to better characterise drug release ( $R^2 > 0.97$  and  $0.99$  for paclitaxel and elacridar, respectively), which is in line with prior research using nanoemulsions [53–55].

*P-Glycoprotein Inhibition*

*Assay*

P-gp-mediated transport has been shown to be inhibited by substances that damage membranes, interfere with ATP binding, or deplete ATP [56,57]. Due to their impact on membranes, polysorbates and other surfactants may block P-gp; nevertheless, the necessary concentrations are often large [40,44,58].P-gpATPase activity was compared with NETri and elacridar-loaded-NETri (E-NETri) after treatment of membranes that express this transporter as evidence that elacridar inclusion enhanced the capacity of NETri to block efflux transporters. E-NETri significantly decreased P-gp activity at 2.5 and 3.5 mg/mL in contrast to the unloaded NETri ( $p < 0.05$ , Two-way ANOVA, Sidak's multiple comparisons post-test) (Figure 4). According to these findings, adding elacridar to NETri enhanced the nanoemulsion's capacity to block P-gp, leading to more noticeable transporter inhibitions at lower nanoemulsion concentrations

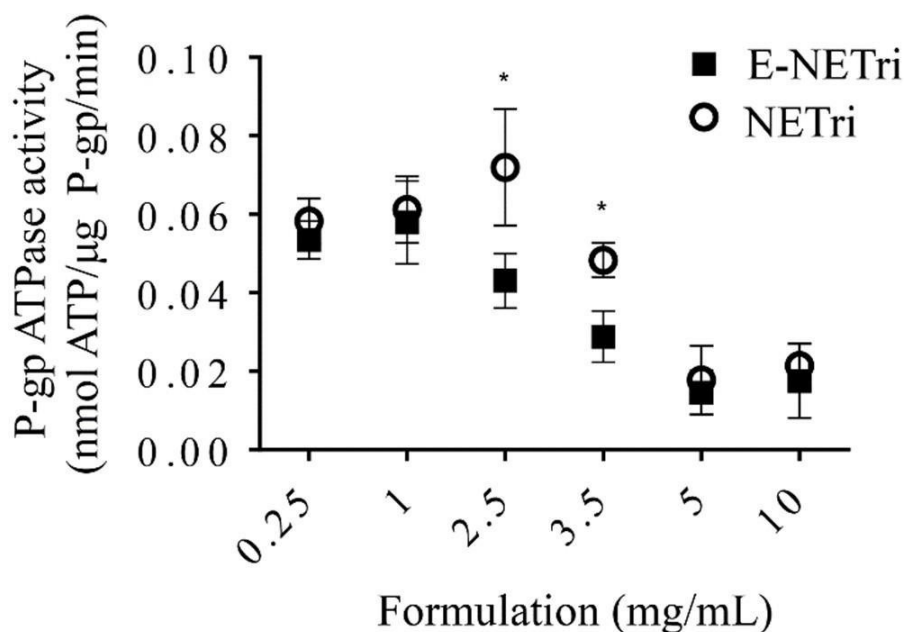


**Figure 4.** Influence of NE concentration on verapamil-induced P-gp ATPase activity. Sidak's statistical test showed significant difference between E-NETri compared to NETri ( $*p < 0.05$ ) at 2.5 and 3.5 mg/mL. Data represented as the mean ± SD, of 3–5 samples.

*Cytotoxicity Evaluation of the Drug-Loaded NETri*

The cytotoxic effects of the drug-loaded NETri were next examined on spheroids and monolayers of breast cancer cells. Since drug incorporation in micro and nanoemulsion affects drug solubility and delivery into cells and tissues [14,59], the experiments were performed to determine whether (i) paclitaxel incorporation in NETri increased its cytotoxic effects compared to the drug solution, and (ii) elacridar incorporation influenced formulation cytotoxicity. Cytotoxicity in Monolayer Cells When compared to the unloaded NETri, the formulation cytotoxicity rose by up to ten times when paclitaxel was added to the chosen nanoemulsion (P-NETri) (Table 2). IC50 results of ~50–60 μM when the drug solution was used showed that the cells were not extremely sensitive to

paclitaxel. Other groups reported similar paclitaxel IC50 values in breast cancer cell lines [60]. Incorporating paclitaxel into NETri (P-NETri) increased cytotoxicity when compared to paclitaxel solution (P-Sol), albeit the strength of this impact varied depending on the type of cell (Figure 5). IC50 values decreased by around 2.5 to 12.4 times, with MDA-MB-231 cells showing the most noticeable decrease. The inclusion of HA in the nanoemulsion may serve to increase paclitaxel cytotoxicity in cells that express CD44 receptors, since this effect may be connected to the triple negative cells' greater expression of CD44 receptors in comparison to MCF-7 cells [33,61].

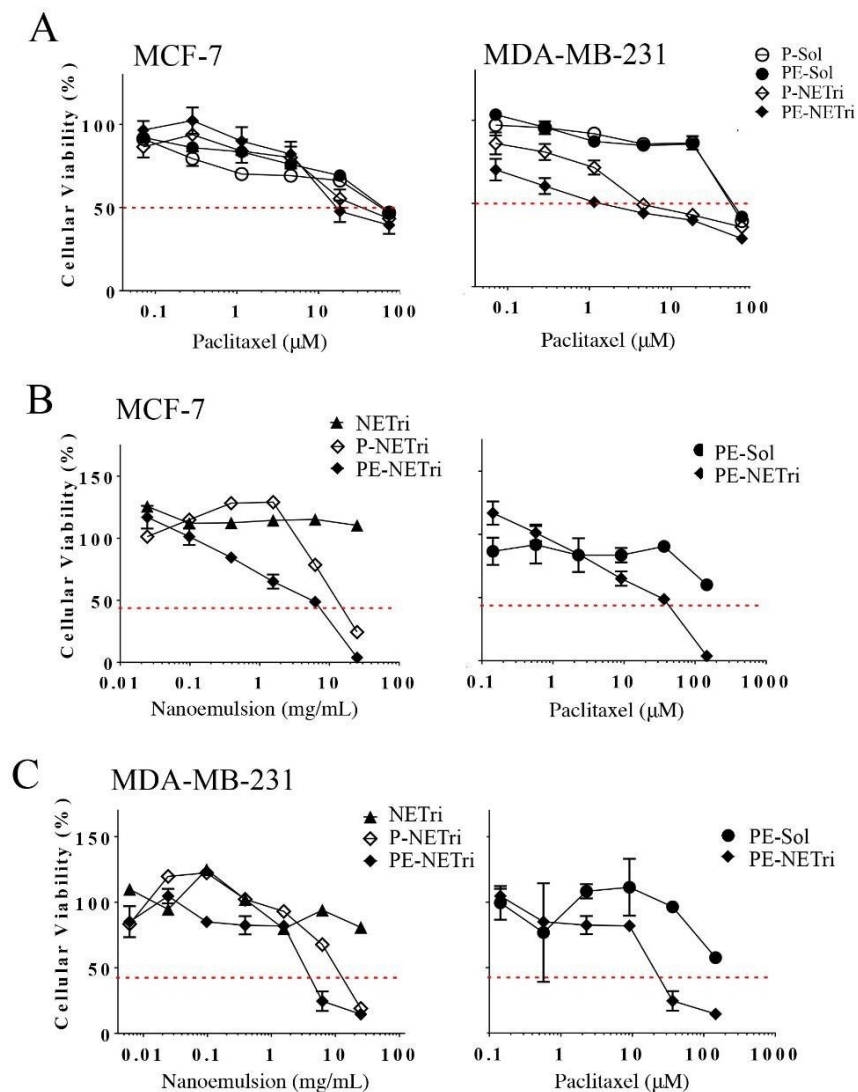


**Figure 5.** Influence of the concentration of paclitaxel solution (P-Sol), paclitaxel + elacridar solution (PE-Sol), unloaded nanoemulsion (NETri), paclitaxel-loaded (P-NETri), or paclitaxel + elacridar-loaded nanoemulsion (PE-NETri) on the viability of breast cancer cells in 2D and 3D (spheroids) culture. (A) Viability of MCF-7 and MDA-MB-231 cells in monolayer (2D culture) after 48 h of treatment. Data are represented as the mean  $\pm$  SD,  $n=12-15$  in 3-4 separate experiments; (B) viability of MCF-7 spheroids after 72 h of treatment, (C) viability of MDA-MB-231 spheroids after 72 h of treatment. Data are represented as the mean  $\pm$  SD,  $n = 3-4$ . The concentrations of the formulation and paclitaxel are presented in mg/mL and  $\mu\text{M}$ , respectively.



Elacridar did not significantly alter cytotoxicity and IC50 values in any of the cell lines, according to a comparison of paclitaxel solution with and without it (P-Sol and PE-Sol) (Figure 5A and Table 2). However, compared to P-NETri, co-incorporation of paclitaxel and elacridar in NETri resulted in a 1.6–2.9-fold decrease in the viability of MCF-7 and MDA-MB-231 cells, indicating a potential impact of the NE on paclitaxel (and not only elacridar) delivery. These findings suggest that, in comparison to its solution, the formulation is an appropriate approach for co-delivery of paclitaxel elacridar, boosting paclitaxel cytotoxicity.

**Cytotoxicity in Spheroids**

After it was shown that adding paclitaxel to the nanoemulsion increased its cytotoxicity in cell monolayers, the impact of the formulation on MDA-MB-231 and MCF-7 spheroids was

evaluated. Spheroids are used as 3D models because they have been shown to replicate the in vivo cellular milieu more accurately than monolayer cultures. Even at the greatest concentration tested, the unloaded NETri did not cause the viability of MDA-MB-231 or MCF-7 spheroids to drop to less than 80% (Figure 5B,C, and Table 3). This may be explained by the fact that spheres have more complex structures and more constant diffusional barriers than cell monolayers. Both spheroids' formulation cytotoxicity was enhanced by the addition of paclitaxel to the nanoemulsion (P-NETri); IC50 values of 6.6 and 11.1 μM were reported (Table 3). Co-incorporating elacridar with paclitaxel resulted in further increases; the most noticeable impact was shown in MDA-MB-231 spheroids (3.2-fold decrease in the formulation IC50 compared to P-NETri, Table 3).

**Table 3.** Values of IC50 related to 3D cell culture of MCF-7 and MDA-MB-231.

IC50	MCF-7		MDA-MB-231	
	mg/mL of NE	μM of P	mg/mL of NE	μM of P
NETri	-	-	-	-
PE-Sol	-	-	-	-
P-NETri	6.6	38.5	11.1	64.8
PE-NETri	3.9	23.1	3.4	19.7

The PE solution did not lower spheroid viability to 50% or below, just as the unloaded formulation did. Co-incorporating paclitaxel and elacridar in NETri resulted in a change of the viability curves to the left, indicating enhanced cytotoxicity. Once again, MDA-MB-231 spheroids had the lowest IC50 value (19.7 μM) (Table 3). As shown in Figure 6, the spheroids treated with PE-NETri at its IC50 value darkened, and more loose cells and cell debris were visible in the medium following the 72-hour treatment than either the spheroids treated with the unloaded NETri (at the same concentration) or the spheroids treated before treatment. Comparable outcomes were found for MCF-7 cells.

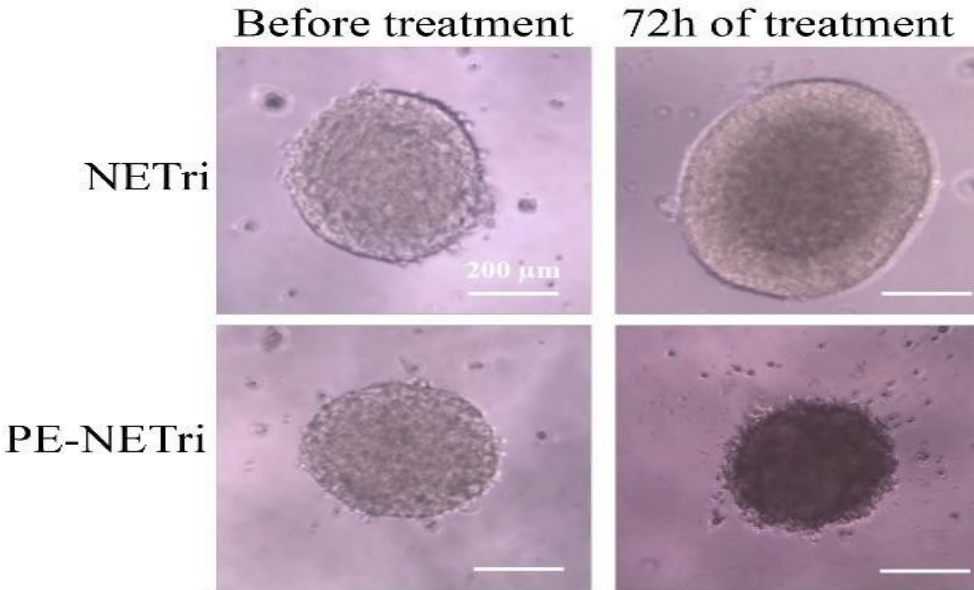


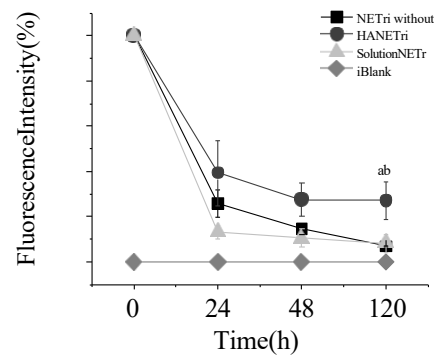
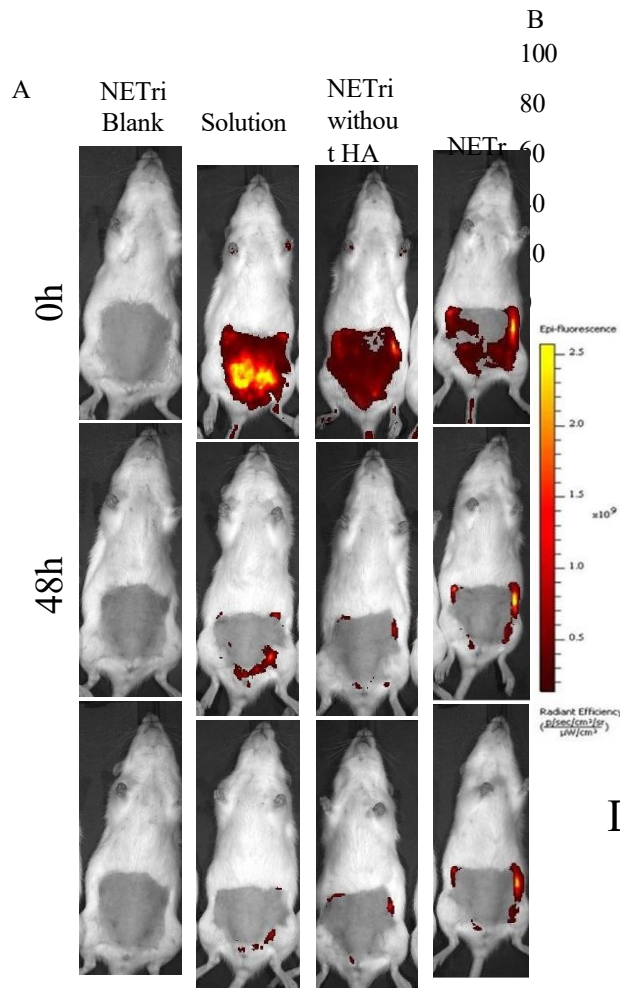
**Figure 6.** MDA-MB-231 spheroids observed before and after treatment for 72h with the unloaded NETri or PE-NETri at the IC50 value of PE-NETri.

*In Vivo Mammary Retention of a Fluorescent Marker*

A rhodamine-loaded NE was used to assess if the presence of HA impacted tissue retention and whether the nanoemulsion could localise chemicals in the mammary tissue in vivo after intraductal injection.

For 120 hours, the mammary tissue's rhodamine retention was observed. Since there was no fluorescence labelling from the unloaded (rhodamine-free) NETri, it was evident that the presence of rhodamine in the tissue is what causes the signals (Figure 7). On the day of injection, the mammary tissue was fluorescently stained by intraductal administration of rhodamine solution, rhodamine-loaded NETri (including HA), or rhodamine-loaded nanoemulsion without HA. Staining decreased throughout the course of five days regardless of the kind of therapy, however the reduction was more noticeable when using the solution than NETri (Figure 7A). More precisely, rhodamine-loaded NETri and rhodamine solution decreased staining to 35 and 10% of the original intensity, respectively. This resulted in a staining signal that was more

than three times larger utilising NETri ( $p < 0.05$ ) after 120 hours (Figure 7B). These findings point to the potential advantages of combining bioadhesive nanoemulsions with intraductal administration to increase mammary retention. It's interesting to note that staining from NETri without HA was inferior to NETri (which contains HA at 0.25%) and comparable to the fluorochrome solution ( $p > 0.05$ , Two-way ANOVA, and post hoc Tuckey). This highlights the significance of HA in the formulation and its function in enhancing tissue retention. When we removed the breast tissue and examined tissue staining under a fluorescence microscope, the fluorochrome was still in the tissue, mostly in the ducts and surrounding tissues, despite the fact that the rhodamine signal's strength had diminished after five days. The rhodamine signal remained strong in the NE-HA group (Figure 7C).



D

120h

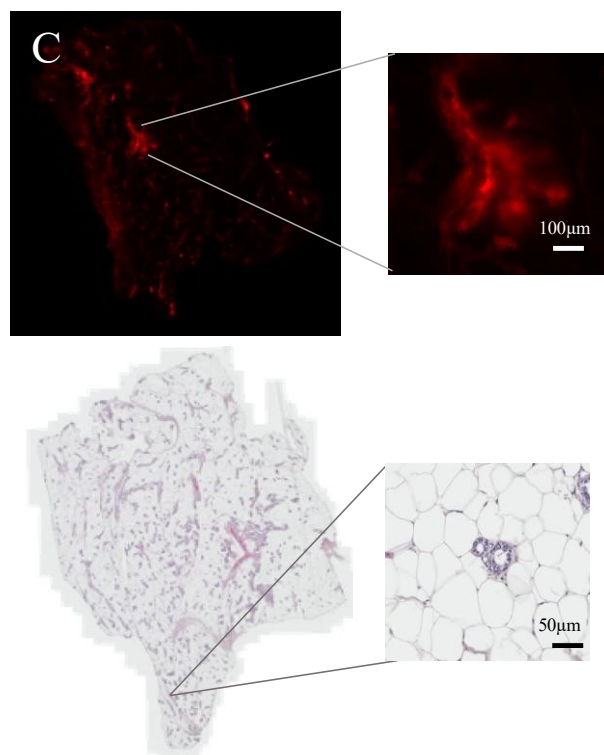


**Figure 7.**

in vivo mammary retention of the fluorescent marker rhodamine over 120h after intraductal (ID) administration and histological changes.

(A) Representative images of the fluorescence signal in female rats treated with 0.5% rhodamine solution, NETri without HA and NETri loaded with 0.5% rhodamine; unloaded NETri was employed for autofluorescence assessment. (B) Decay of fluorescence intensity along 120h after ID administration.

Data are represented as the mean  $\pm$  SD. Tukey's statistical test ( $n=3-4$ ) showed significant difference between NETri compared to the solution ( $a = p < 0.01$ ) and NETri compared to the NETri without HA ( $b = p < 0.01$ ). (C) Fluorescent signal remaining in the breast tissue after 120h of ID administration of NETri containing 0.5% rhodamine. The zoom shows a ductal tree with its alveoli, suggesting that the fluorescent signal came from inside the ducts. Bar = 100  $\mu$ m. (D) Representative image of the mammary tissue after ID administration of the NETri obtained by optical microscopy. Bar = 100  $\mu$ m.

According to the features of the ducts and tissue organisation, including the epithelium, adipose tissue with unilocular adipocytes, and connective tissue (stroma) that surrounds the ducts, ductules (smaller ducts), and alveoli, none of the formulations produced inflammatory symptoms in the breast tissue [62]. There were lymph nodes, blood arteries, nerves, and smooth muscle fibres in the adipose tissue [62], but there were no unusually high lymphocytes or other indications of inflammatory cell infiltration. There were no abnormalities or lesions seen in the duct and alveolar lumen, which was likewise free of secretions or cells.

(Fig. 7D). Although additional assessment of histological changes in the mammary tissue and other biochemical parameters (like liver function) after longer treatment periods would be required to ensure safety, the animals' lack of changes in weight, locomotion, and leukocyte count (Supplementary Table S1) supports the formulation's potential safety when administered through the intraductal route.

## Discussion

The chemotherapeutic drug paclitaxel has been used extensively to treat solid tumours, but its potential to cause a number of serious side effects is still a drawback that drives the quest for alternative delivery methods and administration routes in order to preserve effectiveness and reduce systemic toxicity [63,64]. Our goal in this work was to create a nanoemulsion that would allow paclitaxel and elacridar to be delivered intraductally and co-incorporated. In this work, the composition was carefully chosen and optimised to allow the acquisition of certain features that are pertinent to intraductal administration and the treatment of breast cancer. Our understanding of how formulation makeup affects cytotoxicity was aided by cell culture research. We showed that tributyrin and PA at 0.5–1% enhanced formulation cytotoxicity, but only in MCF-7 cells. In this cell line, Migotto et al. also found cytotoxicity increase mediated by tributyrin, which resulted in a decrease in the IC50 of an emulsions of

more than 80% [8]. The current work not only supports the triglyceride's capacity for cytotoxicity, but it also shows that this impact is shown at eight-fold lower concentrations when it is added to the NE. In regards to PA, Yeruva and associates showed that by inducing G0/G1 arrest, sensitising cells, and lowering IC50 values of cisplatin, PA treatment decreased viability and enhanced apoptosis in MDA-MB-231 and MCF-7 by 33.7% and 12.6%, respectively [65]. Given that the observed IC50 of PA to suppress the growth of MDA-MB-213 cells was 1.5 mM, increases in PA content in the NE may be relevant to further enhance cytotoxicity in these cells. The PA content in the cell culture medium would only approach this amount at the maximum NE concentration (50 mg/mL). NETri was more stable after drug loading, even though tributyrin and PA-containing nanoemulsions had comparable cytotoxicity. To the best of our knowledge, no prior reports have examined the connection between the presence of PA and decreased NE stability. Depending on the kind of surfactant, Fengetal found that certain D-limonene-loaded nanoemulsions showed instability (creaming, bigger droplets, and high Turbiscan Stability Index) [66]. Perillyl alcohol, an almonene component, may need different kinds of surfactant systems in order to create stable nanoemulsions. Since it has been shown that drug loading into phospholipid-stabilized emulsified systems and the compartment in which they localise might affect stability, it is also worthwhile to take into account the function of drug localisation in the nanoemulsion [50]. As was already noted, lipophilic medications (such as paclitaxel and elacridar) may be found in several parts of the nanoemulsion: dispersed/dissolved in the aqueous phase, entrapped/dissolved in the oil droplets, and in the surfactant interface [49,50,67]. Drug localisation at interfaces may affect surfactant activity and, therefore, droplet stability because of the tiny droplet size and high interface-to-core ratio [50]. It is reasonable to assume that PA and elacridar dissolve differently because PA is less lipophilic than tributyrin (logP of 1.9 versus a predicted logP of 2.9 for tributyrin) [68]. This could favour drug incorporation at the surfactant interface in the presence of PA, affecting surfactant function and nanoemulsion stability. Additionally, tributyrin's increased lipophilicity may have made NETri more stable since nanoemulsions are susceptible to Ostwald ripening, and decreasing the oil phase's aqueous solubility helps to inhibit this process [69]. The addition of paclitaxel to NETri enhances cytotoxicity. Despite its many harmful side effects, paclitaxel is regarded as an efficient chemotherapeutic medication that is used as a cornerstone in the treatment of early or metastatic breast cancer. For this reason, nanocarriers have been regularly researched to enhance cytotoxicity and cancer cell targeting. For instance, Bernabeu and Researchers found that adding paclitaxel to nanoparticles functionalised with TPGS-b-PCL decreased their IC50 by almost 60% [60]. When the medication was added to a microemulsion, Pepe et al. observed a two-fold decrease in the IC50 value in basal cell cancer cells [59]. In SK-MEL-19 cells, Carvalho et al. showed that adding paclitaxel to a nanoemulsion decreased its IC50 by four times [16]. A research by Bu and associates also shown that, in comparison to the drug solution, a nanoemulsion based on TPGS, Tween 80, and medium chain triglyceride decreased the IC50 in MCF-7/ADR cells by 18.9 times [70]. An enhanced solubility of lipophilic medicines in the culture medium and their distribution to cells and tissues have been linked to the cytotoxicity enhancement mediated by anoemulsified carriers [16,71]. More effective passive

diffusion—caused by the presence of surfactants and other penetration enhancers as nanoemulsion components—and/or specialised processes may be responsible for the enhanced delivery [72,73]. According to earlier research, phosphatidylcholine and surfactants (such so-called sorbates) may function as sorption enhancers, changing the structure and permeability of biological barriers and enhancing drug diffusion through them [72,74–76]. It has been proposed that the presence of polysorbates and poloxamers in neurocarriers might cause endocytosis across the blood–brain barrier because of their affinity for lipoproteins and other biological molecules [77]. Furthermore, hyaluronic acid has been identified as a CD44 ligand that may cause cell internalisation by endocytosis mediated by CD44 [78]. We have previously shown using differential scanning calorimetry that the addition of HA raised the glass transition temperature ( $T_g$ ) in nanoemulsions from  $-45$  to  $-36^\circ\text{C}$ , the melting peak temperature ( $T_{\text{peak}}$ ) from  $-0.8$  to  $+1.4^\circ\text{C}$ , and the enthalpy of fusion ( $\Delta H_{\text{fus}}$ ) from 214.7 to 243.0 J/g. These findings imply that HA can influence the mobility of water near interfaces [12]. These findings suggest that the interface or an area near it may contain at least some of the polysaccharide content. Previous studies using cationic micelles reported that hyaluronan chains do not penetrate into the interior of micelles formed with decyl- and dodecyltrimethyl-ammonium bromides, and charged groups of hyaluronic acid might act as counterions [79,80], even though the types of interactions between HA and surfactants forming these nanoemulsions were not further investigated. Furthermore, the domains created by the hydroxyl groups of hyaluronate were drawn to the hydrophilic headgroups of non-ionic and anionic surfactants (such sodium dodecyl sulfonate) [80]. Additionally, it was proposed that phospholipid-based aggregates' hydrophobic surface may interact with HA by binding the hydrophobic sections of the HA chain [81,82]. Further supporting the advantages of nanoemulsified systems for the solubilisation and administration of lipophilic chemicals like paclitaxel and elacridar, we also showed that paclitaxel and elacridar together in the nanoemulsion, but not as a solution, enhanced its cytotoxicity. Given that elacridar's presence in the nanoemulsion did not impair its capacity to inhibit P-gp, the increase in paclitaxel cytotoxicity may be linked to enhanced elacridar cell uptake and efflux transporter inhibition. It has been shown that MCF-7 and MDA-MB-231 cells express P-gp, but at far lower levels than resistant cells, which may indicate that elacridar helps to block efflux [83,84]. Other studies have showed the advantages of co-loading nanocarriers with paclitaxel and elacridar to enhance cytotoxicity, block efflux, and reverse multidrug resistance. For instance, Tonbul et al. found that when elacridar (100 nM) was co-encapsulated, the cellular viability dropped by almost 77%, but paclitaxel-loaded nanoparticles alone at 50  $\mu\text{M}$  showed nearly no cytotoxic impact in the EMT6/AR1.0 mouse mammary tumour cell line [85]. Future research will evaluate the cytotoxicity of the formulation in breast cancer cells that are resistant to paclitaxel (our group has been working on the creation of these cells). Clinically, it would be ideal for chemotherapeutic drugs to be associated with inhibitors of efflux transporters in order to increase their effectiveness. However, because transporters are not only expressed in tumours, increasing the cytotoxic effect of paclitaxel may result in a proportionate increase in systemic adverse effects and toxicity [86]. This issue can be resolved by local



administration into the mammary ducts. The main reason hyaluronic acid (HA) was added to the nanoemulsion was because of its bioadhesive qualities [12,87,88], however this naturally occurring anionic polymer has other functions. As previously stated, it is a ligand of CD44; due to its overexpression in a number of cancer types, it is a potential target to improve the specificity of therapies directed at tumour cells [12,89]. Since the NE without HA promoted retention that was comparable to the solution, we showed *in vivo* that the inclusion of HA in the nanoemulsion was necessary to extend the local retention of rhodamine. Our findings contradict those of Barbault-Foucheretal, who showed that HA had the ability to adhere to mucosa in an ocular drug delivery system based on poly-ε-caprolactone nanospheres. This might be because HA does not adhere to the precorneal mucin layer covalently [87]. Mucins play a crucial role in protecting and lubricating ducts coated with epithelium [90], and their presence in the mammary ducts is a significant characteristic of the pathway that supports the use of bioadhesive nanocarriers. To our knowledge, this is the first proof that HA presence in the nanoemulsion was really required for this effect, and that a four-fold lower HA content was enough. We have previously shown that HA-modified nanoemulsions were able to extend breast tissue retention of a hydrophilic probe [12]. The formulation did not alter the breast tissue's histological features, indicating that it does not encourage local adverse responses throughout the study period.

### 3. Materials and Methods

#### Materials

Croda Health Care, located in Edison, New Jersey, USA, generously provided the tripartin. 2-dipalmitoyl-sn-glycero-3-phosphoethanolamine (DPPE) and soy phosphaticholine (PC) were acquired from AvantiPolar Lipids (Alabaster, AL, USA), while propylene glycol and glycerol were acquired from Synth (São Paulo, SP, Brazil). The supplier of paclitaxel and elacridar was Cayman Chemical Company (Ann Arbor, MI, USA). Sigma (St. Louis, MO, USA) provided the polysorbate 80, tetrazolium dye 3-(4,5-dimethylthiazol-2-yl)-2,5-diphenyltetrazoliumbromide (MTT), trichomerin (Tri), and perillyl alcohol (PA). Other specific chemicals and their corresponding methods are detailed. Unless otherwise noted, ultrapure water was used.

#### Nanoemulsion Development

The oil phase and surfactant combination (PC:DPPE:polysorbate80:propyleneglycol:glycerol3:0.2:1:0.5:0.45, w/w/w/w/w) at 1:1(w/w, making up 20% of the formulation) were combined to create nanoemulsions. Because DPPE has been shown to promote the absorption of nanoparticles by cancer cells, we included phospholipids in the surfactant blend to decrease surfactant-based irritation [91,92]. The aqueous phase (80% of the formulation) was then washed to 40 °C and added to the combination while vortex mixing for 30 seconds. The formulations were then sonicated for 10 minutes at a rate of 58 seconds on and 30 seconds off in an ice bath (VCX-500, Sonics, Newtown, CT, USA). The NanoZS90 (Zetasizer, Malvern, UK) apparatus was used to measure the particle diameter, polydispersity index (PDI), and zeta potential after a 1:100 (w/w) nanoemulsion dilution with water. An R/S Plus controlled stress rheometer with the RC75-1 geometry (Brookfield Engineering Laboratories,

Middleboro, MA, USA) and a controlled temperature of 25°C was used to examine the rheological behaviour of the formulations. In the studies, shear rates ranging up to 2000s<sup>-1</sup> were used [48]. As explained in the next subsections, this nanoemulsion preparation procedure was modified twice in order to evaluate the impact of the composition of the aqueous and oil phases on the nanoemulsion properties.

#### Influence of Oil Phase on NE Formation

Three kinds of oil phases were studied in order to evaluate the impact of tributyrin (Tri) and perillyl alcohol (PA) on emulsion characteristics: tricaprylin and tricaprylin with either tributyrin or perillyl alcohol (with a final concentration in the mixture ranging from 0.5 to 5%). nanoemulsion). Before adding the aqueous phase and sonicating, the oil phase was mixed with the surfactant mixture. Before further testing, homogeneous formulations were stored at room temperature and shielded from light for up to seven days to see if they remained preliminary stable (showing no symptoms of aggregation, phase separation, or screaming). Aqueous Phase Influence on NE Formation Next, it was determined how the NE properties were affected by the addition of hyaluronic acid (HA, low molecular weight, 10 KDa, Lifecore Biomedical, Chaska, MA, USA). Before being incorporated into the aqueous phase, it was dissolved in PBS to achieve final concentrations of 0.125, 0.25, and 0.5%. As stated, the formulas were sonicated. Before undergoing further testing, homogeneous formulations were stored at room temperature and shielded from light for seven days to see whether they remained stable. Short-Term Stability, Drug Incorporation, and Release Before the aqueous phase addition, paclitaxel and elacridar were dissolved in specific oil phase: surfactant mixes. Based on earlier research on drug solubility in micro and nanoemulsions [16,27,59], two concentrations of paclitaxel (0.5% and 1%) and of elacridar (0.1% and 0.07%) were examined, and their impact on the physicochemical properties was evaluated. Using NanoZS90 (Zetasizer, Malvern, UK) equipment, droplet diameter, polydispersity index (PDI), and zeta potential were measured after a 1:100 (w/w) dilution of the nanoemulsions with water. Selected unloaded NEs and those with elacridar were chosen based on their characteristics. Paclitaxel (0.5% w/w, 5.9 mM) and (0.07% w/w, 1.2 mM) underwent a short-term stability test. For ninety days, the three batches of formulations were stored at room temperature (maintained by air conditioning set at 25 °C), shielded from light, and examined under a microscope (Leica, Wetzlar, Germany) and visually for indications of aggregation, phase separation, or creaming. Additionally, as previously mentioned, droplet size, PDI, and zeta potential were evaluated. The formulation was placed in the recipient compartment of Franz diffusion cells in small dialysis bags (14,000 Dacutoff, Sigma-Aldrich, St. Louis, MO, USA) in phosphate buffered saline (PBS) + 1% polysorbate 80, pH7.4, at 37°C under stirring (150 rpm) as previously described [93] to assess whether paclitaxel and elacridar were released from the chosen NE. At predeter, aliquots of the receptor phase (0.25 mL) were taken out. mined time intervals (3–24 hours), and a Shimadzu HPLC equipment with a Phenomenex C18 column was used to analyse the samples [16,59]. At 228 nm using mobile phase, which is constituted of 55:45 (v/v), Paclitaxel was measured. water and acetonitrile at a flow rate of 20 µL of



injection at room temperature (25 °C) at a rate of 1.0 mL/min. Using a mobile phase made of acetonitrile:water (60:40, v/v) at a rate of 1 mL/min and UV detection at 249 nm, elacridar was tested at a temperature of 20 µL at room temperature (25°C). Drug quantification was done using calibration curves of elacridar (2–20 µg/mL,  $R^2 > 0.993$ ) or paclitaxel (0.2–100 µg/mL,  $R^2 > 0.995$ ) produced in methanol.  $Q = Q_0 + K_0 t$ , Higuchi kinetics ( $Q = K_h t^{1/2}$ ), and first-order kinetics ( $\log Q_t = -K t/2.303 + \log Q_0$ ), where  $Q_0$  is the starting amount of drug in the solution,  $K_0$  is a zero-order kinetic constant,  $K_h$  is the Higuchi dissolving constant, and  $Q_{tr}$  is the absolute amount of drug release in time (in hours) [93]. After 30 days of storing the chosen nanoemulsion (NETri) at room temperature (kept by air conditioning set at 25°C) and shielded from light, we also measured the drug content to determine if the medications would be degraded. Drug concentrations of 7 (elacridar) or 10 (paclitaxel) µg/mL were theoretically obtained by HPLC following NE dilutions (triplicates, separate dilutions for paclitaxel and elacridar as the former was integrated at a greater level) with methanol. Tests for Cytotoxicity: 2D and 3D Models Assessment of Cytotoxicity in Cell Monolayers (2D Model) The impact of nanoemulsion composition and drug inclusion on the viability of two breast cancer cell lines (MCF-7 and MDA-MB-231, ATCC, Manassas, VA, USA) was investigated since component selection affects drug delivery and cytotoxicity [44,94]. The cells were kept in culture in DMEM/F12 medium supplemented with 10% Antibiotics and foetal bovine serum at 37°C in a 5% CO<sub>2</sub> atmosphere. When they arrived The cells were trypsinised at around 80% confluence and then plated at a density of 10,000 cells/well on 96-well culture plates. For 48 hours [95,96], cells were exposed to the chosen unloaded NEs, drug-loaded formulations, or paclitaxel solution at concentrations ranging from 0.07 to 73.2 µM of paclitaxel and 0.006 to 25 mg/mL of formulations. As suggested by Mosmann [97], MTT was used to assess cell viability. As controls, untreated cells and cells treated with doxorubicin, PBS (the NE's vehicle), and DMSO (doxorubicin's solvent) were used. Using trypan blue, the concentration required to lower cell viability to 50% (IC<sub>50</sub>) was verified. In short, cells were treated with the nanoemulsions at the IC<sub>50</sub> as established by MTT; after treatment, they were counted in Neubauer's chamber and stained with 0.4% trypan blue (1:1v/v). Trypan blue-stained cells were deemed nonviable. Assessment of Cytotoxicity in Spheroids (3D Model)

MCF-7 and MDA-MB-231 spheroids were acquired by the use of the liquid overlay approach, which prevents adherence to the plate surface [10,93]. As a result, 96-well microplates were made, with 50 µL of 1% agarose solution in each well [93]. Five x 10<sup>3</sup> cells per well were then seeded, centrifuged for seven minutes at 1000 RPM, and then incubated at 37°C in an incubator with 5% CO<sub>2</sub> [93].

Serial dilutions of paclitaxel solution (beginning at 73 µM), unloaded NE (NE without paclitaxel or elacridar), NE with paclitaxel, or NE were used to treat the spheroids.

for 72 hours with elacridar and paclitaxel. According to the manufacturer's instructions, spheroids were next sent to a viability evaluation (CellTiterGlo® 3D, Promega, Madison, WI, USA) using luminescent measurement of ATP levels.

This was followed by an absorbance measurement in a luminescence reader (560 nm). Assay for Glycoprotein-PI Inhibition

The Pro-Glo™ Assay (Promega, Madison, WI, USA) and standardised recombinant P-gp membranes were used to measure the transporter activity in order to determine if elacridar inclusion altered the NE ability to block ATP hydrolysis and P-gp-mediated transport, as previously reported [27,44]. Elacridar-containing and elacridar-free nanoemulsions were evaluated at final concentrations between 0.25 and 10 mg/mL. Verapamil, an L-type calcium channel blocker, stimulated membranes expressing P-gp, while sodium orthovanadate (Na<sub>3</sub>VO<sub>4</sub>) served as a background control and a gauge of P-gp-independent ATPase activity to inhibit P-gp ATPase. An alluminometer was used to measure the NE's P-gp inhibitory effects, and the results were translated to P-gp ATPase activity based on a calibration curve made using 0.375–3 mM ATP standards. Based on ATP levels in membranes treated with Na<sub>3</sub>VO<sub>4</sub> and untreated membranes, the baseline activity was, for comparison, 0.07 nmol consumed ATP/µg P-gp/minute. A Fluorescent Marker's In Vivo Mammary Retention Mediated by the Selected Nanoemulsion

In the past, female Wistar rats (7–8 weeks) were kept in housing where they had unrestricted access to food and water. The animal chamber was kept between 22 and 23°C with a light-dark cycle (12:12 hours). Every experiment was carried out in compliance with the National Council for Animal Experimentation's (CONCEA) criteria and authorised by the University of São Paulo's Animal Care and Use Committee (protocol number #69/2016, São Paulo, Brazil). Rats were anaesthetised before to treatment by inhaling isoflurane (2–2.5%) to eliminate abdominal hair with the help of

VEET® cream, the duct orifice was exposed by gently rubbing the region with cotton soaked in alcohol [8,12]. The rhodamine (0.5%) nanoemulsions, which were made by dissolving the dye (0.5%, w/w) in the surfactant:oil phase combination, were intraductally delivered (20 µL) using a 33G needle (Hamilton, Bonaduz, Switzerland) connected to a 0.1 mL syringe. Three pairs of nipples were chosen based on the ease of access. The IVIS Spectrum system (Perkin-Elmer Life Sciences, Waltham, MA, USA) at CEFAP-ICB-USP was used to measure the in vivo fluorescence intensity for 120 hours.

With a binning value of 8–2 and an exposure length of 0.5 s, the fluorescence intensity at the mammary tissue was measured using an absorption filter at 465–540 nm. Following the experiment, the mammary tissue was either (i) embedded in optimal tissue organisation or (ii) fixed for histology to evaluate NE-mediated changes in tissue organisation.

Using a cryostat (Leica CM 1850 UV) to cut a 9 µm piece of the compound to determine the persistence of the rhodamine-loaded NE fluorescent signal in the mammary

ducts. Tissues were then examined. Axioscan 7 (Germany, Zeiss). Analyses of Statistics

The ANOVA test and either the Tukey or Sidak post-hoc test (GraphPad Prism software, San Diego, CA, USA) were used

to statistically analyse the data. When  $p < 0.05$ , values were deemed substantially different.

## Conclusions

In this work, we optimised the composition of the nanoemulsion for the co-incorporation of elacridar and paclitaxel. We demonstrated that the chosen nanocarrier (i) exhibited appropriate properties and short-term stability, and (ii) enhanced the cytotoxicity of paclitaxel, which was further enhanced in 2D and 3D models by the addition of elacridar. Additionally, elacridar decreased the amount of nanoemulsion required to block P-gpATPase activity. To extend the in vivo retention of rhodamine (incorporated in NEGRI), nanoemulsion modification with HA was crucial. These findings show that even in triple negative breast cancer cell lines, the nanoemulsion created here can carry paclitaxel and elacridar to cancer cells and increase its lethal impact. This finding's primary significance is that there are few therapy choices available for triple negative breast cancer, which opens up new avenues for the study of novel therapeutic approaches for the condition.

## References

- Solin, L.J. Management of Ductal Carcinoma In Situ (DCIS) of the Breast: Present Approaches and Future Directions. *Curr. Oncol. Rep.* **2019**, *21*, 33. [CrossRef] [PubMed]
- Groen, E.J.; Elshof, L.E.; Visser, L.L.; Rutgers, E.J.; Winter-Warnars, H.A.; Lips, E.H.; Wesseling, J. Finding the balance between over- and under-treatment of ductal carcinoma in situ (DCIS). *Breast Edinb. Scotl.* **2017**, *31*, 274–283. [CrossRef] [PubMed]
- Wang, G.; Chen, C.; Pai, P.; Korangath, P.; Sun, S.; Merino, V.F.; Yuan, J.; Li, S.; Nie, G.; Stearns, V. Intraductal fulvestrant for therapy of ER $\alpha$ -positive ductal carcinoma in situ of the breast: A preclinical study. *Carcinogenesis* **2019**, *40*, 903–913. [CrossRef] [PubMed]
- Chun, Y.S.; Bisht, S.; Chenna, V.; Pramanik, D.; Yoshida, T.; Hong, S.-M.; de Wilde, R.F.; Zhang, Z.; Huso, D.L.; Zhao, M. Intraductal administration of a polymeric nanoparticle formulation of curcumin (NanoCurc) significantly attenuates incidence of mammary tumors in a rodent chemical carcinogenesis model: Implications for breast cancer chemoprevention in at-risk populations. *Carcinogenesis* **2012**, *33*, 2242–2249. [CrossRef]
- Stearns, V.; Mori, T.; Jacobs, L.K.; Khouri, N.F.; Gabrielson, E.; Yoshida, T.; Kominsky, S.L.; Huso, D.L.; Jeter, S.; Powers, P.; et al. Preclinical and clinical evaluation of intraductally administered agents in early breast cancer. *Sci. Transl. Med.* **2011**, *3*, 106ra108. [CrossRef]
- Wang, G.; Kumar, A.; Ding, W.; Korangath, P.; Bera, T.; Wei, J.; Pai, P.; Gabrielson, K.; Pastan, I.; Sukumar, S. Intraductal administration of transferrin receptor-targeted immunotoxin clears ductal carcinoma in situ in mouse models of breast cancer—preclinical study. *Proc. Natl. Acad. Sci. USA* **2022**, *119*, e2200200119. [CrossRef]
- Singh, Y.; Gao, D.; Gu, Z.; Li, S.; Rivera, K.A.; Stein, S.; Love, S.; Sinko, P.J. Influence of molecular size on the retention of polymeric nanocarrier diagnostic agents in breast ducts. *Pharm. Res.* **2012**, *29*, 2377–2388. [CrossRef]
- Migotto, A.; Carvalho, V.F.M.; Salata, G.C.; da Silva, F.W.M.; Yan, C.Y.I.; Ishida, K.; Costa-Lotufo, L.V.; Steiner, A.A.; Lopes, L.B. Multifunctional nanoemulsions for intraductal delivery as a new platform for local treatment of breast cancer. *Drug Deliv.* **2018**, *25*, 654–667. [CrossRef]
- Al-Zubaydi, F.; Gao, D.; Kakkar, D.; Li, S.; Adler, D.; Holloway, J.; Szekely, Z.; Gu, Z.; Chan, N.; Kumar, S.; et al. Breast intraductal nanoformulations for treating ductal carcinoma in situ: Exploring metal-ion complexation to slow cyclopirox release, enhance mammary persistence and efficacy. *J. Control. Release* **2020**, *323*, 71–82. [CrossRef]
- Dartora, V.F.C.; Salata, G.C.; Passos, J.S.; Branco, P.C.; Silveira, E.; Steiner, A.A.; Costa-Lotufo, L.V.; Lopes, L.B. Hyaluronic acid nanoemulsions improve paclitaxine cytotoxicity in 2D and 3D breast cancer models and reduce tumor development after intraductal administration. *Int. J. Biol. Macromol.* **2022**, *219*, 84–95. [CrossRef]
- Joseph, M.K.; Islam, M.S.; Reineke, J.; Hildreth, M.; Woyengo, T.; Pillatzki, A.; Baride, A.; Perumal, O. Intraductal Drug Delivery to the Breast: Effect of Particle Size and Formulation on Breast Duct and Lymph Node Retention. *Mol. Pharm.* **2019**, *17*, 441–552. [CrossRef] [PubMed]
- Carvalho, V.F.M.; Salata, G.C.; de Matos, J.K.R.; Costa-Fernandez, S.; Chorilli, M.; Steiner, A.A.; de Araujo, G. L.B.; Silveira, E.R.; Costa-Lotufo, L.V.; Lopes, L.B. Optimization of composition and obtention parameters of biocompatible nanoemulsions intended for intraductal administration of paclitaxine (paclitaxine) and mammary tissue targeting. *Int. J. Pharm.* **2019**, *567*, 118460. [CrossRef] [PubMed]
- Ozogul, Y.; Karsli, G.T.; Durmus, M.; Yazgan, H.; Oztop, H.M.; McClements, D.J.; Ozogul, F. Recent developments in
- Giacone, D.V.; Dartora, V.; de Matos, J.K.R.; Passos, J.S.; Miranda, D.A.G.; de Oliveira, E.A.; Silveira, E.R.; Costa-Lotufo, L.V.; Maria-Engler, S.S.; Lopes, L.B. Effect of nanoemulsion modification with chitosan and sodium alginate on the topical delivery and efficacy of the cytotoxic agent paclitaxine in 2D and 3D skin cancer models. *Int. J. Biol. Macromol.* **2020**, *165*, 1055–1065. [CrossRef] [PubMed]
- Sánchez-López, E.; Guerra, M.; Dias-Ferreira, J.; Lopez-Machado, A.; Ettcheto, M.; Cano, A;

- Espina, M.; Camins, A.; Garcia, M.L.; Souto, E.B. Current Applications of Nanoemulsions in Cancer Therapeutics. *Nanomaterials* **2019**, *9*, 821. [[CrossRef](#)] [[PubMed](#)]
16. Carvalho, V.F.M.; Migotto, A.; Giaccone, D.V.; de Lemos, D.P.; Zandoni, T.B.; Maria-Engler, S.S.; Costa-Lotuf, L.V.; Lopes, L.B. Co-encapsulation of paclitaxel and C6 ceramide in tributyrin-containing nanocarriers improve co-localization in the skin and potentiate cytotoxic effects in 2D and 3D models. *Eur. J. Pharm. Sci.* **2017**, *109*, 131–143. [[CrossRef](#)] [[PubMed](#)]
  17. Dosio, F.; Arpicco, S.; Stella, B.; Fattal, E. Hyaluronic acid for anticancer drug and nucleic acid delivery. *Adv. Drug Deliv. Rev.* **2016**, *97*, 204–236. [[CrossRef](#)]
  18. Chan, S.; Friedrichs, K.; Noel, D.; Pintér, T.; Van Belle, S.; Vorobiof, D.; Duarte, R.; Gil Gil, M.; Bodrogi, I.; Murray, E. Prospective randomized trial of docetaxel versus doxorubicin in patients with metastatic breast cancer. *J. Clin. Oncol.* **1999**, *17*, 2341. [[CrossRef](#)]
  19. Evans, T.R.J.; Yellowlees, A.; Foster, E.; Earl, H.; Cameron, D.A.; Hutcheon, A.W.; Coleman, R.E.; Perren, T.; Gallagher, C.J.; Quigley, M. Phase III randomized trial of doxorubicin and docetaxel versus doxorubicin and cyclophosphamide as primary medical therapy in women with breast cancer: An Anglo-Celtic cooperative oncology group study. *J. Clin. Oncol.* **2005**, *23*, 2988–2995. [[CrossRef](#)]
  20. Khanna, C.; Rosenberg, M.; Vail, D.M. A review of paclitaxel and novel formulations including those suitable for use in dogs. *J. Vet. Intern. Med.* **2015**, *29*, 1006–1012. [[CrossRef](#)] [[PubMed](#)]
  21. Priyadarshini, K.; Keerthi, A.U. Paclitaxel against cancer: A short review. *Med. Chem.* **2012**, *2*, 139–141.
  22. Foa, R.; Norton, L.; Seidman, A.D. Taxol (paclitaxel): A novel anti-microtubule agent with remarkable anti-neoplastic activity. *Int. J. Clin. Lab. Res.* **1994**, *24*, 6–14. [[CrossRef](#)] [[PubMed](#)]
  23. Ndungu, J.M.; Lu, Y.J.; Zhu, S.; Yang, C.; Wang, X.; Chen, G.; Shin, D.M.; Snyder, J.P.; Shoji, M.; Sun, A. Targeted Delivery of Paclitaxel to Tumor Cells: Synthesis and In Vitro Evaluation. *J. Med. Chem.* **2010**, *53*, 3127–3132. [[CrossRef](#)] [[PubMed](#)]
  24. McGrogan, B.T.; Gilmartin, B.; Carney, D.N.; McCann, A. Taxanes, microtubules and chemoresistant breast cancer. *Biochim. Biophys. Acta BBA-Rev. Cancer* **2008**, *1785*, 96–132. [[CrossRef](#)] [[PubMed](#)]
  25. Murray, S.; Briasoulis, E.; Linardou, H.; Bafaloukos, D.; Papadimitriou, C. Taxane resistance in breast cancer: Mechanisms, predictive biomarkers and circumvention strategies. *Cancer Treat. Rev.* **2012**, *38*, 890–903. [[CrossRef](#)]
  26. Dash, R.P.; Jayachandra Babu, R.; Srinivas, N.R. Therapeutic Potential and Utility of Elacridar with Respect to P-glycoprotein Inhibition: An Insight from the Published In Vitro, Preclinical and Clinical Studies. *Eur. J. Drug Metab. Pharmacokinet.* **2017**, *42*, 915–933. [[CrossRef](#)] [[PubMed](#)]
  27. Giaccone, D.V.; Carvalho, V.F.M.; Costa, S.K.P.; Lopes, L.B. Evidence That P-glycoprotein Inhibitor (Elacridar)-Loaded Nanocarriers Improve Epidermal Targeting of an Anticancer Drug via Absorptive Cutaneous Transporters Inhibition. *J. Pharm. Sci.* **2018**, *107*, 698–705. [[CrossRef](#)]
  28. Crowell, P.L.; Ayoubi, A.S.; Burke, Y.D. Antitumorogenic effects of limonene and perillyl alcohol against pancreatic and breast cancer. In *Dietary Phytochemicals in Cancer Prevention and Treatment*; Springer: Berlin/Heidelberg, Germany, 1996; pp. 131–136.
  29. Chen, T.C.; Da Fonseca, C.O.; Schönthal, A.H. Preclinical development and clinical use of perillyl alcohol for chemoprevention and cancer therapy. *Am. J. Cancer Res.* **2015**, *5*, 1580.
  30. Chaudhary, S.C.; Alam, M.S.; Siddiqui, M.S.; Athar, M. Perillyl alcohol attenuates Ras-ERK signaling to inhibit murine skin inflammation and tumorigenesis. *Chem.-Biol. Interact.* **2009**, *179*, 145–153. [[CrossRef](#)]
  31. Heidor, R.; Festa Ortega, J.; de Conti, A.; Prates Ong, T.; Salvador Moreno, F. Anticarcinogenic actions of tributyrin, a butyric acid prodrug. *Curr. Drug Targets* **2012**, *13*, 1720–1729. [[CrossRef](#)]
  32. Allison, K.H.; Hammond, M.E.H.; Dowsett, M.; McKernin, S.E.; Carey, L.A.; Fitzgibbons, P.L.; Hayes, D.F.; Lakhani, S.R.; Chavez-MacGregor, M.; Perlmutter, J. Estrogen and progesterone receptor testing in breast cancer: American Society of Clinical Oncology/College of American Pathologists guideline update. *Arch. Pathol. Lab. Med.* **2020**, *144*, 545–563. [[CrossRef](#)] [[PubMed](#)]
  33. Chekhun, S.; Bezdenezhnykh, N.; Shvets, J.; Lukianova, N. Expression of biomarkers related to cell adhesion, metastasis and invasion of breast cancer cell lines of different molecular subtype. *Exp. Oncol.* **2013**, *35*, 174–179. [[PubMed](#)]
  34. Collignon, J.; Lousberg, L.; Schroeder, H.; Jerusalem, G. Triple-negative breast cancer: Treatment challenges and solutions. *Breast Cancer Targets Ther.* **2016**, *8*, 93.
  35. Abumanhal-Masarweh, H.; da Silva, D.; Poley, M.; Zinger, A.; Goldman, E.; Krinsky, N.; Kleiner, R.; Shenbach, G.; Schroeder, J.E.; Shklover, J.; et al. Tailoring the lipid composition of nanoparticles modulates their cellular uptake and affects the viability of triple-negative breast cancer cells. *J. Control. Release* **2019**, *307*, 331–341. [[CrossRef](#)] [[PubMed](#)]
  36. Mojeiko, G.; Apolinário, A.C.; Salata, G.C.; Chorilli, M.; Lopes, L.B. Optimization of nanoemulsified

- systems containing lamellarphases for co-delivery of celecoxib and endoxifen to the skin aiming for breast cancer chemoprevention and treatment. *Colloids Surf. A Physicochem. Eng. Asp.* **2022**, 646, 128901. [[CrossRef](#)]
37. Roethlisberger, D.; Mahler, H.-C.; Altenburger, U.; Pappenberger, A. Ifeuhydricand isotonicdonot work,what areacceptable pHandosmolalityforparenteraldrugdosageforms? *J.Pharm. Sci.* **2017**,106,446–456. [[CrossRef](#)]
38. Laursen, T.; Hansen, B.; Fisker, S. Pain perception after subcutaneous injections of media containing different buffers. *Basic Clin. Pharmacol. Toxicol.* **2006**, 98, 218–221. [[CrossRef](#)]



39. Phelps, J.; Bentley, M.V.; Lopes, L.B. In situ gelling hexagonal phases for sustained release of an anti-addiction drug. *Colloids Surf. B Biointerfaces* **2011**, *87*, 391–398. [[CrossRef](#)]
40. Lo, Y.L. Relationships between the hydrophilic-lipophilic balance values of pharmaceutical excipients and their multidrug resistance modulating effect in Caco-2 cells and rat intestines. *J. Control. Release* **2003**, *90*, 37–48. [[CrossRef](#)]
41. Hosmer, J.M.; Steiner, A.A.; Lopes, L.B. Lamellar liquid crystalline phases for cutaneous delivery of Paclitaxel: Impact of the monoglyceride. *Pharm. Res.* **2013**, *30*, 694–706. [[CrossRef](#)]
42. Bernhofer, L.P.; Barkovic, S.; Appa, Y.; Martin, K.M. IL-1 $\alpha$  and IL-1 $\beta$  secretion from epidermal equivalents and the prediction of the irritation potential of mild soap and surfactant-based consumer products. *Toxicol. Vitro* **1999**, *13*, 231–239. [[CrossRef](#)]
43. Hosmer, J.; Reed, R.; Bentley, M.V.; Nornoo, A.; Lopes, L.B. Microemulsions containing medium-chain glycerides as transdermal delivery systems for hydrophilic and hydrophobic drugs. *AAPS Pharm Sci Tech* **2009**, *10*, 589–596. [[CrossRef](#)][[PubMed](#)]
44. Pepe, D.; McCall, M.; Zheng, H.; Lopes, L.B. Protein transduction domain-containing microemulsions as cutaneous delivery systems for an anticancer agent. *J. Pharm. Sci.* **2013**, *102*, 1476–1487. [[CrossRef](#)]
45. Vater, C.; Bosch, L.; Mitter, A.; Göls, T.; Seiser, S.; Heiss, E.; Elbe-Bürger, A.; Wirth, M.; Valenta, C.; Klang, V. Lecithin-based nanoemulsions of traditional herbal wound healing agents and their effect on human skin cells. *Eur. J. Pharm. Biopharm.* **2022**, *170*, 1–9. [[CrossRef](#)][[PubMed](#)]
46. Mojeiko, G.; de Brito, M.; Salata, G.C.; Lopes, L.B. Combination of microneedles and microemulsions to increase celecoxib topical delivery for potential application in chemoprevention of breast cancer. *Int. J. Pharm.* **2019**, *560*, 365–376. [[CrossRef](#)][[PubMed](#)]
47. Lopes, L.B.; Scarpa, M.V.; Pereira, N.L.; de Oliveira, L.C.; Oliveira, A.G. Interaction of sodium diclofenac with freeze-dried soya phosphatidylcholine and unilamellar liposomes. *Rev. Bras. Cienc. Farm.* **2006**, *42*, 8. [[CrossRef](#)]
48. Apolinário, A.C.; Salata, G.C.; de Souza, M.M.; Chorilli, M.; Lopes, L.B. Rethinking Breast Cancer Chemoprevention: Technological Advantages and Enhanced Performance of a Nanoethosomal-Based Hydrogel for Topical Administration of Fenretinide. *AAPS Pharm Sci Tech.* **2022**, *23*, 104. [[CrossRef](#)]
49. Apolinário, A.C.; Hauschke, L.; Nunes, J.R.; Lopes, L.B. Towards nanoformulations for skin delivery of poorly soluble API: What does indeed matter? *J. Drug Deliv. Sci. Technol.* **2020**, *60*, 102045. [[CrossRef](#)]
50. Francke, N.M.; Bunjes, H. Influence of drug loading on the physical stability of phospholipid-stabilised colloidal lipid emulsions. *Int. J. Pharm.* **2020**, *2*, 100060. [[CrossRef](#)]
51. di Cagno, M.; Luppi, B. Drug “supersaturation” states induced by polymeric micelles and liposomes: A mechanistic investigation into permeability enhancements. *Eur. J. Pharm. Sci.* **2013**, *48*, 775–780. [[CrossRef](#)]
52. Fatouros, D.G.; Antimisiaris, S.G. Effect of amphiphilic drugs on the stability and zeta-potential of their liposome formulations: A study with prednisolone, diazepam, and griseofulvin. *J. Colloid Interface Sci.* **2002**, *251*, 271–277. [[CrossRef](#)][[PubMed](#)]
53. Sakulku, U.; Nuchuchua, O.; Uwongyart, N.; Puttipatkhachorn, S.; Soottitawat, A.; Ruktanonchai, U. Characterization and mosquito repellent activity of citronella oil nanoemulsion. *Int. J. Pharm.* **2009**, *372*, 105–111. [[CrossRef](#)][[PubMed](#)]
54. Taha, E.I.; Al-Saidan, S.; Samy, A.M.; Khan, M.A. Preparation and in vitro characterization of self-nanoemulsified drug delivery system (SNEDDS) of all-trans-retinol acetate. *Int. J. Pharm.* **2004**, *285*, 109–119. [[CrossRef](#)][[PubMed](#)]
55. de Almeida Borges, V.R.; Simon, A.; Sena, A.R.C.; Cabral, L.M.; de Sousa, V.P. Nanoemulsion containing dapsone for topical administration: A study of in vitro release and epidermal permeation. *Int. J. Nanomed.* **2013**, *8*, 535.
56. Demina, T.; Grozdova, I.; Krylova, O.; Zhirnov, A.; Istratov, V.; Frey, H.; Kautz, H.; Melik-Nubarov, N. Relationship between the structure of amphiphilic copolymers and their ability to disturb lipid bilayers. *Biochemistry* **2005**, *44*, 4042–4054. [[CrossRef](#)]
57. Regev, R.; Assaraf, Y.G.; Eytan, G.D. Membrane fluidization by ether, other anesthetics, and certain agents abolishes P-glycoprotein ATPase activity and modulates efflux from multidrug-resistant cells. *Eur. J. Biochem.* **1999**, *259*, 18–24. [[CrossRef](#)]
58. Barta, C.A.; Sachs-Barrable, K.; Feng, F.; Wasan, K.M. Effects of monoglycerides on P-glycoprotein: Modulation of the activity and expression in Caco-2 cell monolayers. *Mol. Pharm.* **2008**, *5*, 863–875. [[CrossRef](#)]
59. Pepe, D.; Carvalho, V.F.; McCall, M.; de Lemos, D.P.; Lopes, L.B. Transport in nanocarriers improves skin localization and antitumor activity of paclitaxel. *Int. J. Nanomed.* **2016**, *11*, 2009–2019. [[CrossRef](#)]
60. Bernabeu, E.; Gonzalez, L.; Legaspi, M.J.; Moreton, M.A.; Chiappetta, D.A. Paclitaxel-loaded TPGS-b-PCL nanoparticles: In vitro cytotoxicity and



- cellular uptake in MCF-7 and MDA-MB-231 cells versus mPEG-b-PCL nanoparticles and Abraxane®. *J. Nanosci. Nanotechnol.* **2016**, *16*, 160–170. [[CrossRef](#)]
61. Sheridan, C.; Kishimoto, H.; Fuchs, R.K.; Mehrotra, S.; Bhat-Nakshatri, P.; Turner, C.H.; Goulet, R.; Badve, S.; Nakshatri, H. CD44<sup>+</sup>/CD24<sup>-</sup>breast cancer cells exhibit enhanced invasive properties: An early step necessary for metastasis. *Breast Cancer Res.* **2006**, *8*, R59. [[CrossRef](#)]
  62. Masso-Welch, P.A.; Darcy, K.M.; Stangle-Castor, N.C.; Ip, M.M. A developmental atlas of rat mammary gland histology. *J. Mammary Gland Biol. Neoplasia* **2000**, *5*, 165–185. [[CrossRef](#)][[PubMed](#)]
  63. Liu, Q.; Zhao, D.; Zhu, X.; Chen, H.; Yang, Y.; Xu, J.; Zhang, Q.; Fan, A.; Li, N.; Guo, C.; et al. Co-loaded Nanoparticles of Paclitaxel and Piperlongumine for Enhancing Synergistic Antitumor Activities and Reducing Toxicity. *J. Pharm. Sci.* **2017**, *106*, 3066–3075. [[CrossRef](#)][[PubMed](#)]
  64. Nornoo, A.O.; Zheng, H.; Lopes, L.B.; Johnson-Restrepo, B.; Kannan, K.; Reed, R. Oral microemulsions of paclitaxel: In Situ and pharmacokinetic studies. *Eur. J. Pharm. Biopharm.* **2009**, *71*, 310–317. [[CrossRef](#)][[PubMed](#)]
  65. Yeruva, L.; Hall, C.; Elegbede, J.A.; Carper, S.W. Perillyl alcohol and methyl jasmonates sensitize cancer cells to cisplatin. *Anti-Cancer Drugs* **2010**, *21*, 1–9. [[CrossRef](#)]
  66. Feng, J.; Wang, R.; Chen, Z.; Zhang, S.; Yuan, S.; Cao, H.; Jafari, S.M.; Yang, W. Formulation optimization of D-limonene-loaded nanoemulsions as a natural and efficient biopesticide. *Colloids Surf. A Physicochem. Eng. Asp.* **2020**, *596*, 124746. [[CrossRef](#)]
  67. Francke, N.M.; Bunjes, H. Drug localization and its effect on the physical stability of poloxamer 188-stabilized colloidal lipid emulsions. *Int. J. Pharm.* **2021**, *599*, 120394. [[CrossRef](#)][[PubMed](#)]
  68. Miastkowska, M.; Śliwa, P. Influence of Terpene Type on the Release from an O/W Nanoemulsion: Experimental and Theoretical Studies. *Molecules* **2020**, *25*, 2747. [[CrossRef](#)]
  69. Wooster, T.J.; Golding, M.; Sanguansri, P. Impact of oil type on nanoemulsion formation and Ostwald ripening stability. *Langmuir* **2008**, *24*, 12758–12765. [[CrossRef](#)]
  70. Bu, H.; He, X.; Zhang, Z.; Yin, Q.; Yu, H.; Li, Y. A TPGS-incorporating nanoemulsion of paclitaxel circumvents drug resistance in breast cancer. *Int. J. Pharm.* **2014**, *471*, 206–213. [[CrossRef](#)]
  71. Stover, T.; Kester, M. Liposomal delivery enhances short-chain ceramide-induced apoptosis of breast cancer cells. *J. Pharm. Exp.* **2003**, *307*, 468–475. [[CrossRef](#)]
  72. Ganta, S.; Deshpande, D.; Korde, A.; Amiji, M. A review of multifunctional nanoemulsion systems to overcome oral and CNS drug delivery barriers. *Mol. Membr. Biol.* **2010**, *27*, 260–273. [[CrossRef](#)][[PubMed](#)]
  73. Gao, F.; Zhang, Z.; Bu, H.; Huang, Y.; Gao, Z.; Shen, J.; Zhao, C.; Li, Y. Nanoemulsion improves the oral absorption of candesartan cilexetil in rats: Performance and mechanism. *J. Control. Release* **2011**, *149*, 168–174. [[CrossRef](#)][[PubMed](#)]
  74. Jena, L.; McErlean, E.; McCarthy, H. Delivery across the blood-brain barrier: Nanomedicine for glioblastoma multiforme. *Drug Deliv. Transl. Res.* **2020**, *10*, 304–318. [[CrossRef](#)][[PubMed](#)]
  75. Kim, C.; Shim, J.; Han, S.; Chang, I. The skin-permeation-enhancing effect of phosphatidylcholine: Caffeine as a model active ingredient. *J. Cosmet. Sci.* **2002**, *53*, 363–374. [[PubMed](#)]
  76. Hathout, R.M.; Mansour, S.; Mortada, N.D.; Geneidi, A.S.; Guy, R.H. Uptake of microemulsion components into the stratum corneum and their molecular effects on skin barrier function. *Mol. Pharm.* **2010**, *7*, 1266–1273. [[CrossRef](#)][[PubMed](#)]
  77. Kreuter, J. Influence of the surface properties on nano-particle-mediated transport of drugs to the brain. *J. Nanosci. Nanotechnol.* **2004**, *4*, 484–488. [[CrossRef](#)][[PubMed](#)]
  78. Huang, G.; Huang, H. Application of hyaluronic acid as carriers in drug delivery. *Drug Deliv.* **2018**, *25*, 766–772. [[CrossRef](#)]
  79. Holínková, P.; Mravec, F.; Venerová, T.; Chang, C.-H.; Pekar, M. Hyaluronan interactions with cationic surfactants—Insights from fluorescence resonance energy transfer and anisotropy techniques. *Int. J. Biol. Macromol.* **2022**, *211*, 107–115. [[CrossRef](#)]
  80. Yin, D.-S.; Yang, W.-Y.; Ge, Z.-Q.; Yuan, Y.-J. A fluorescence study of sodium hyaluronate/surfactant interactions in aqueous media. *Carbohydr. Res.* **2005**, *340*, 1201–1206. [[CrossRef](#)][[PubMed](#)]
  81. Scott, J.E.; Cummings, C.; Brass, A.; Chen, Y. Secondary and tertiary structures of hyaluronan in aqueous solution, investigated by rotary shadowing-electron microscopy and computer simulation. Hyaluronan is a very efficient network-forming polymer. *Biochem. J.* **1991**, *274*, 699–705. [[CrossRef](#)]
  82. El Kechai, N.; Geiger, S.; Fallacara, A.; Cañero Infante, I.; Nicolas, V.; Ferrary, E.; Huang, N.; Bochet, A.; Agnely, F. Mixtures of hyaluronic acid and liposomes for drug delivery: Phase behavior, microstructure and mobility of liposomes. *Int. J. Pharm.* **2017**, *523*, 246–259. [[CrossRef](#)][[PubMed](#)]

83. Chen, J.; Lu, L.; Wang, H.; Dai, L.; Zhang, P. PKD2 mediate multi-drug resistance in breast cancer cells through modulation of P-glycoprotein expression. *Cancer Lett.* **2011**, *300*, 48–56. [[CrossRef](#)] [[PubMed](#)]
84. Chen, T.; Wang, C.; Liu, Q.; Meng, Q.; Sun, H.; Huo, X.; Sun, P.; Peng, J.; Liu, Z.; Yang, X. Dasatinib reverses the multidrug resistance of breast cancer MCF-7 cells to doxorubicin by downregulating P-gp expression via inhibiting the activation of ERK signaling pathway. *Cancer Biol. Ther.* **2015**, *16*, 106–114. [[CrossRef](#)]
85. Tonbul, H.; Sahin, A.; Tavukcuoglu, E.; Esendagli, G.; Capan, Y. Combination drug delivery with actively-targeted PLGA nanoparticles to overcome multidrug resistance in breast cancer. *J. Drug Deliv. Sci. Technol.* **2019**, *54*, 101380. [[CrossRef](#)]
86. Palmeira, A.; Sousa, E.; Vasconcelos, M.H.; Pinto, M.M. Three decades of P-gp inhibitors: Skimming through several generations and scaffolds. *Curr. Med. Chem.* **2012**, *19*, 1946–2025. [[CrossRef](#)]
87. Barbault-Foucher, S.; Gref, R.; Russo, P.; Guechot, J.; Bochot, A. Design of poly-ε-caprolactone nanospheres coated with bioadhesive hyaluronic acid for ocular delivery. *J. Control. Release* **2002**, *83*, 365–375. [[CrossRef](#)]
88. Oh, S.; Wilcox, M.; Pearson, J.P.; Borrós, S. Optimal design for studying mucoadhesive polymer interaction with gastric mucin using a quartz crystal microbalance with dissipation (QCM-D): Comparison of two different mucin origins. *Eur. J. Pharm. Biopharm.* **2015**, *96*, 477–483. [[CrossRef](#)]
89. Yang, X.-Y.; Li, Y.-X.; Li, M.; Zhang, L.; Feng, L.-X.; Zhang, N. Hyaluronic acid-coated nanostructured lipid carriers for targeting paclitaxel to cancer. *Cancer Lett.* **2013**, *334*, 338–345. [[CrossRef](#)]
90. Mukhopadhyay, P.; Chakraborty, S.; Ponnusamy, M.P.; Lakshmanan, I.; Jain, M.; Batra, S.K. Mucins in the pathogenesis of breast cancer: Implications in diagnosis, prognosis and therapy. *Biochim. Biophys. Acta BBA-Rev. Cancer* **2011**, *1815*, 224–240. [[CrossRef](#)]
91. Waiczies, S.; Lepore, S.; Sydow, K.; Drechsler, S.; Ku, M.-C.; Martin, C.; Lorenz, D.; Schütz, I.; Reimann, H.M.; Purfürst, B. Anchoring dipalmitoyl phosphoethanolamine to nanoparticles boosts cellular uptake and fluorine-19 magnetic resonance signal. *Sci. Rep.* **2015**, *5*, 8427. [[CrossRef](#)]
92. Han, S.; Liu, Y.; Nie, X.; Xu, Q.; Jiao, F.; Li, W.; Zhao, Y.; Wu, Y.; Chen, C. Efficient Delivery of Antitumor Drug to the Nuclei of Tumor Cells by Amphiphilic Biodegradable Poly(L-Aspartic Acid-co-Lactic Acid)/DPPE Co-Polymer Nanoparticles. *Small* **2012**, *8*, 1596–1606. [[CrossRef](#)] [[PubMed](#)]
93. Salata, G.C.; Malagó, I.D.; Carvalho Dartora, V.F.M.; Marçal Pessoa, A.F.; Fantini, M.C.A.; Costa, S.K.P.; Machado-Neto, J.A.; Lopes, L.B. Microemulsion for Prolonged Release of Fenretinide in the Mammary Tissue and Prevention of Breast Cancer Development. *Mol. Pharm.* **2021**, *18*, 3401–3417. [[CrossRef](#)] [[PubMed](#)]
94. Silva, A.M.; Martins-Gomes, C.; Coutinho, T.E.; Figueiro, J.F.; Sanchez-Lopez, E.; Pashirova, T.N.; Andreani, T.; Souto, E.B. Soft cationic nanoparticles for drug delivery: Production and cytotoxicity of solid lipid nanoparticles (SLNs). *Appl. Sci.* **2019**, *9*, 4438. [[CrossRef](#)]
95. Yang, M.-Y.; Wang, C.-J.; Chen, N.-F.; Ho, W.-H.; Lu, F.-J.; Tseng, T.-H. Luteolin enhances paclitaxel-induced apoptosis in human breast cancer MDA-MB-231 cells by blocking STAT3. *Chem.-Biol. Interact.* **2014**, *213*, 60–68. [[CrossRef](#)] [[PubMed](#)]
96. Vali, F.; Changizi, V.; Safa, M. Synergistic apoptotic effect of crocin and paclitaxel or crocin and radiation on MCF-7 cells, a type of breast cancer cell line. *Int. J. Breast Cancer* **2015**, *2015*, 139349. [[CrossRef](#)] [[PubMed](#)]
97. Mosmann, T. Rapid colorimetric assay for cellular growth and survival: Application to proliferation and cytotoxicity assays. *J. Immunol. Methods* **1983**, *65*, 55–63. [[CrossRef](#)]